The diversification of lynx lineage during the Plio-Pleistocene——evidence from a new small *Lynx* from Longdan, Gansu Province, China

Running title: A new small *Lynx* from China

Qigao Jianzuo [a,b,c]*, Lu Li [b,c,d], Joan Madurell-Malapeira [e], Shiqi Wang [b,c], Shijie Li [b,c,d], Jiao Fu [b,c,d], Shanqin Chen [f]

a Key Laboratory of Orogenic Belts and Crustal Evolution, School of Earth and Space Sciences, Peking University, 5 Yiheyuan Road, Beijing, 100871

b Key Laboratory of Vertebrate Evolution and Human Origins of Chinese Academy of Sciences, Institute of Vertebrate Paleontology and Paleoanthropology, Chinese Academy of Sciences, Beijing, 10044, China

c CAS Center for Excellence in Life and Paleoenvironment, Beijing, 100044, China;

d University of Chinese Academy of Sciences, Beijing, 100049, China

e Institut Català de Paleontologia, Universitat Autònoma de Barcelona, Cerdanyola del Vallès, 08193. Barcelona. Spain.

f Hezheng Paleozoological Museum, Hezheng, 731200, China

Abstract: A new small-sized lynx from Longdan, Gansu Province, *Lynx hei* sp. nov., is described in this study. The new species displays the characteristic *Lynx* generic traits, e.g., distinct buccal grooves in the upper canine, presence of anterior groove in the upper canine, absence of the P2, and moderately developed mastoid process, but it is markedly smaller than the previously described *L. issiodorensis* specimens from the same site, and is also overall smaller than most living species, comparable to *Lynx rufus* in size. The new species has a relatively wide and deep zygomatic arch, similar to that of living *L. lynx*, *L. pardinus*, *L. canadensis* but wider than that of *L. rufus*. Our phylogenetic analyses suggest that *L. hei* falls within the crown group *Lynx*, being the sister group to *L. rufus*, or less probably to be a sister group to *L. issiodorensis* + three other living species of *Lynx*. The Plio-Pleistocene *L. issiodorensis* is supported as the ancestor of *L. lynx*, *L. pardinus* and *L. canadensis*. Our phylogenetic study suggests that *Lynx* diversification over the Plio-Pleistocene is first achieved by body size differentiation putatively forced by intraspecific competition with other carnivorans, and later followed by morphological divergence.

Key Word: *Lynx*, diversification, Pleistocene, eastern Asia

Introduction

The genus *Lynx* includes several medium-sized cat species with Holarctic distribution (Sunquist and Sunquist, 2002; Bellani, 2019). Four modern species are recognized in the genus, i.e., Eurasian lynx *Lynx lynx*, Iberian lynx *Lynx pardinus*, Canadian lynx *Lynx canadensis*, and bobcat *Lynx rufus*. The first three species are adaptive to dense forest in the temperate and subarctic regions (Tumlison, 1987; Heptner, 1992; Sunquist and Sunquist, 2002; Poole, 2003; Bellani, 2019), whereas *L. rufus* is more like a generalist, although preferring forest environment when available (Lovallo and Anderson, 1996; Sunquist and Sunquist, 2002; Chamberlain et al., 2003). *L. rufus* is different from other species in both morphology and habitat, whereas the rest three species are less well distinguished (Werdelin, 1981; Tumlison, 1987). Recent phylogeny of multilocus data and genomic scale (Johnson et al., 2006; Li et al., 2016), both supported the first divergence of *L. rufus* during the middle part of the Pliocene, followed by *L. canadensis* during the middle Early Pleistocene, and lastly *L. pardinus* and *L. lynx* during the late Early Pleistocene.

As a largely temperate lineage, *Lynx* has one of the best fossil records among Felinae (Werdelin, 1981). The discovery of the fossil material of *Lynx* can be dated back to the early 19th century, i.e. *Felis issiodorensis* (Croizet and Jobert, 1828). More specimens assigned to the *Lynx* genus were later described in Asia (Teilhard de Chardin and Leroy, 1945), North America (Schultz and Martin, 1972), and even Africa (Hendey, 1974; Geraads, 1980, 2016).

Lynx issiodorensis represents the best-recorded and widely spread fossil *Lynx* from the latest Pliocene to Early Pleistocene (Werdelin, 1981; Kurtén and Werdelin, 1984). In Europe, *L. issiodorensis* gradually evolved to the now endangered Iberian species *Lynx pardinus*

(Werdelin, 1981; Boscaini et al., 2016; Mecozzi et al., 2021), whereas *Lynx lynx* probably evolved in Asia population of *L. issiodorensis*, and did not appear in Europe until the Late Pleistocene (Werdelin, 1981; Mecozzi et al., 2021). However, the records of *Lynx* in Eastern Asia Early Pleistocene were found in a few localities, best represented the material from Longdan, Linxia Basin (Qiu et al., 2004). Materials from Longdan were referred to *Lynx shansius* in previous works (Qiu et al., 2004), here *L. shansius* is considered a junior subjective synonym of *L. issiodorensis* following the interpretation of Kurtén and Werdelin (1984).

In this study, we study a new cranium from Longdan, Linxia Basin (Fig. 1, for detailed geological background, see Qiu et al., 2004). This new cranium is distinctly smaller than those of *L. issiodorensis* from the same locality, and the same taxon from Europe, further displaying characteristic *Lynx* traits, representing a previously unknown form and provide key information to understand the early diversification of this iconic Holarctic felid genus.

Materials and methods

The fossil material described in this study is housed in Hezheng Paleozoological Museum (HM). Fossil and living Felidae specimens (including living species of Felidae, as well as fossil *L. issiodorensis* from both Europe and Asia) housed in AMNH, USNM, IGF, IVPP, IOZ, KIZ have been observed for comparison.

The anatomical terms of the cranial anatomical terms of Jayne (1898) on the cat are followed with additional modification as in Qiu et al. (2014). For the craniodental measurement elements, see Fig. 2 for detail.

Our phylogenetic analysis is based on a new morphological matrix, partially from that of Salles (1992) and Werdelin and Flink (2018), including 87 characters for 23 taxa. The matrix is edited using software Mesquite 3.4 (Maddison and Maddison, 2021). The phylogenetic analyses of Maximum Parsimony using software TNT 1.5 (Goloboff et al., 2008; Goloboff and Catalano, 2016) and Bayes Inference using software Mrbayes 3.2.7 (Huelsenbeck and Ronquist, 2001; Ronquist et al., 2012b) were performed. All analyses were set for 4 chains, including three cold chains and one hot chain. Two independent runs were performed, each 10 million generations. Constraint on the lineage of the living species using the backbone from phylogeny inferred from genomic data (Johnson et al., 2006; Li et al., 2016) was used. See the *Comparison and Discussion* section for more detailed settings.

Institutional Abbreviations—AMNH FM fossil mammal collection of the American Museum of Natural History, New York, USA**; AMNH M** mammalian collection of the American Museum of Natural History, New York, USA**; HMV** Hezheng Paleozoological Museum, Hezheng, China; **IGF,** Natural History Museum of Firenze, Italy; **IOZ** Institute of Zoology, Chinese Academy of Science, Beijing, China**; IVPP** Institute of Vertebrate Paleontology and Paleoanthropology, Chinese Academy of Sciences, Beijing, China**; KIZ** Kunming Institute of Zoology, Chinese Academy of Sciences, Kunming, China**; USNM** Smithsonian National Museum of Natural History, Washington DC, USA

Anatomical Abbreviations—BW blade width of the P4 (width across the paracone posterior to the protocone)**; H** height**; L** length; **L1** skull total length; **L2** skull condylobasal length; **L3** skull basilar length; **LDP** diastema between the C-P3; **LT** toothrow length from C-P4; **M/m**

upper/lower molar**; Lme** metacone length**; P/p** upper/lower premolar**; Lpa** parastyle length**; W** width; **W1** zygomatic width; **W2** rostrum width across P4/M1; **W3** rostrum width across the canine.

Results

Order Carnivora Bowdich (1821)

Family Felidae Batsch (1788)

Subfamily Felinae Batsch (1788)

Lynx Kerr (1792)

Lynx hei sp. nov.

(Fig. 3)

Referred specimen—Type specimen HMV2010, almost complete cranium.

Measurements—Table 1

Diagnosis —small-sized lynx with similar overall size to that of living *Lynx rufus*. Rostrum relatively narrow compared with most *Lynx* species. Postorbital process of frontal small. Sagittal crest anteroposteriorly long and weak. Palate narrow. Basisphenoid-basioccipital bone narrow. Upper canine with distinct anterior groove. P2 absent. P3 main cusp high in buccal view. P4 with moderately sized protocone, without buccal groove.

Etymology—In honor to Mr. Wen He, the former curator of Hezheng Museum, who has contributed to the fossil collection and management in Linxia Basin.

Type locality—Longdan, Linxia Basin, Gansu Province, China.

Distribution and chronology—So far known from the early Early Pleistocene in Linxia

Basin (ca. 2.4-2.2Ma).

Description—The cranium is complete, but slightly dorsal-ventrally compressed, so the ventro-dorsal height of this cranium is not original, but the width of the cranium is weakly affected. Judging from the dental wear (apex of the P3 slightly worn) and development of sagittal crest, the individual represents a full adult.

Dorsal view (Fig. 3C) The rostrum is relatively narrower than most other species of *Lynx*. There is not distinct postcanine constriction, but the rostrum gets slightly narrower backward. The forehead is slightly wider than the rostrum. The postorbital process of the frontal is distinct but not strong. The temporal ridges unit into the sagittal crest at the point posterior to the frontal-parietal suture. The lambdoid crest is well developed. **Lateral view (Fig. 3A)** The anterior contour of the naris opening is concave. The highest point of the cranium is located slightly behind the level of the postorbital process of the frontal in lateral view, in the anterior part of the cranium. The sagittal crest is low. The lateral contour of the C-P3 diastema is distinctly dorsally concave. The infraorbital foramen is located at the level of the mesial border of the P3. The anterior border of the orbit is located at the level of the P3 main cusp. The zygomatic arch has a uniform height and is slightly dorsally arched. The postorbital process of the jugal is distinct. The central ridge in the jugal is located around at the middle line of the bone. The mastoid process is distinct. **Ventral view (Fig. 3B)** The incisor row is nearly straight. The palate is relatively narrow for a lynx. The toothrow gets wider backward. The anterior border of the palatine is located at the level of the P3. The bony choana extends distinctly posterior to the M1. The preglenoid process is relatively weak. The foramen ovale is located medially to the glenoid fossa. The auditory bullae are large, whereas the

basisphenoid-basioccipital between the bullae is narrow. The posterior lacerated foramen is located in the same fossa as the hypoglossal foramen.

Dentition The incisors are relatively small. The I1 and I2 are in a similar size, whereas the I3 is distinctly larger. There are two strong vertical grooves in the buccal side of the canine. A slightly weaker vertical groove is present in the anterior side of the tooth. There is no P2 in the left, and a tiny root, which seems to be DP2, is present in the right side. The P3 main cusp is high crowned in buccal view. There is no mesial accessory cusp, whereas the distal accessory cusp and posterior cingulum are well developed. There is weak distolingual convexity in the P3. The P4 has a straight buccal border. There is no vertical groove in the buccal side of the tooth. The ectoparastyle is absent. The parastyle is relatively short. The protocone is moderate in size, and anteriorly located. The M1 is small and transversely elongated.

Comparison and discussion

The characteristic craniodental traits of genus *Lynx*

The most widely known trait for *Lynx* genus is the stable absence of the P2 (Werdelin, 1981). We observed this trait in other felids based on observation of large collection in AMNH and USNM. The P2 is nearly always present in *Panthera* but is sometimes absent in *Neofelis* and *Prionailurus bengalensis*. The P2 seems to be frequently absent in some species of *Leopardus* and in *Pardofelis marmorata*, and *Caracal caracal*. It is absent in all species of *Lynx* we have observed, and all *L. issiodorensis* from Longdan, Gansu Province, and Caozhuang, Shouyang, Shanxi Province, but in two crania from the Mazegou Formation of

the Yushe Basin (Late Pliocene), it is present, though very small (probably DP2). Therefore, the absence of the P2, if taken alone, is not diagnostic for the genus *Lynx*, as several other felids regularly lack this tooth. The presence of the P2, however, suggests the felid is not very likely to be a *Lynx*.

Furthermore, the upper canines of *Lynx* genus display another discriminant character. In its buccal surface, two very deep vertical grooves are present in all living species of *Lynx* (Fig. 4). We studied a large sample of living felid species and found that such deep grooves are not shown by other feline cats, e.g., *Caracal* or *Leptailurus*, except some species of *Leopardus*, e.g., *Le. pardalis*. More interestingly, there is a distinct groove at the anterior side of the canine, just buccal to the anterior ridge of the canine. We check through the living felid species, and again, this groove is absent in all cats except most species of *Leopardus*. The grooves in the canine, therefore, provide more useful evidence to judge whether a cat could belong to *Lynx* genus.

The extant lynxes, except for *L. canadensis*, seldom develops mesial accessory cusp in the P3. It is also absent for all *L. issiodorensis* from Longdan we observed and rarely present in European *L. issiodorensis* and Early Pleistocene *L. pardinus* (Fig. 5). This trait is variable in many felids, e.g., *Leptailurus serval*, *Caracal caracal*, *Leopardus* spp., *Prionailurus* spp., and *Felis* spp. The widest part of the tooth lies at the level around the main cusp/distal accessory cusp boundary (which means the distal side of the tooth is wider) in all species of living *Lynx* except *L. rufus*. In the latter species, the widest part is often more anteriorly near the apex of the main cusp. In *Leopardus* spp. and *Prionailurus viverrinus*, it is more common to see the widest part lies anteriorly, and this point lies posteriorly in *Prionailurus*

194 *bengalensis*, *Catopuma temminckii*, *Pardofelis marmorata*, but quite variable in *Leptailurus*
195 *serval*, and *Caracal caracal* et al. Therefore, these two P3 traits only provide limited
196 evidence for genus judgment but could be used in species inference.
197 The P4 protocone of all living species of *Lynx* is often somewhat reduced in size (Fig.
198 5). This trait is commonly seen in *L. lynx* and *L. pardinus*, and less often seen in *L.*
199 *canadensis* and *L. rufus*. In *L. issiodorensis*, the protocone is also often slightly reduced in
200 size. A small preparastyle is quite common in all three living species, whereas in *L. rufus*, this
201 small cusp is present in around the half specimens we observed. In *L. issiodorensis*, this cusp
202 is also often present. Of particular interest, we noticed that in *L. issiodorensis* (both the Late
203 Pliocene and Early Pleistocene populations from Europe and Asia) there are distinct vertical
204 buccal grooves in most specimens (Fig. 6). This trait, however, is absent the living species
205 (occasionally as shallow imprint in *L. lynx*) or fossil *L. pardinus*. We regard this trait as an
206 important feature for *L. issiodorensis*.
207 Regarding the cranial features, *Lynx* is most characteristic by its broad cranium (wide
208 zygomatic arch, wide rostrum, and wide forehead, see Fig. 7) for a medium-sized cat (smaller
209 cats, e.g., *Felis*, could have an even broader cranium). This trait, however, can only be
210 applied to *L. lynx*, *L. pardinus* and *L. canadensis*, whereas *L. rufus* only has a moderately
211 wide cranium, comparable to that of the similar sized other cats, e.g., *Catopuma temminckii*,
212 *Leopardus pardalis*, and *Leptailurus serval*. In lateral view, the ventral border of the palate in
213 the C-P3 diastema is distinctly dorsally concave in all living species of *Lynx*, as well as in *L.*
214 *issiodorensis*. This trait is generally absent or weak in *Leopardus* spp., *Felis* spp.,
215 *Prionailurus* spp., but present in *Caracal caracal*, *Catopuma temminckii*, *Leptailurus serval*,

Prionailurus viverrinus, though in most of these latter species, the degree of convexity is not so strong as seen in *Lynx*. The zygomatic arch is rather deep and robust in all three species *Lynx* except *L. rufus*. None of the living small to medium-sized cats has such a deep zygomatic arch. The supraorbital process is strong and sharp in all living species of *Lynx* and being variable *L. issiodorensis*. In most feline cats, this process is sharp or variable. The mastoid process is moderately developed in all living species of *Lynx* and *L. issiodorensis*. The mastoid process is weaker in *Felis* spp., and most species of *Prionailurus* spp. but similarly strong in medium-sized felids, e.g., *Caracal caracal*, *Catopuma temminckii*, *Leptailurus serval*, *Prionailurus viverrinus*, so this trait is more likely a size-related character in the feline. The separation of the posterior lactated foramen and hypoglossal foramen is viewed as one of the most important traits to distinguish *L. lynx* from *L. pardinus*, in which the two foramina are located in the same fossa (Boscaini et al., 2016; Mecozzi et al., 2021). Recent observation suggests that the situation in *L. issiodorensis* is the same as in *L. pardinus* (Mecozzi et al., 2021). We checked this trait across the living species as well as in fossil Asian species. The confluence the posterior lactated and hypoglossal foramina is present in most species, in *L. rufus*, *L. hei* as well as *L. pardinus* as previously recognized (Fig. 7). However, it is clearly separated in *L. canadensis*, as in *L. lynx*. *L. issiodorensis* mostly has two foramina in the same fossa. In most other felids, these two foramina are in the same fossa, and this state is likely the primitive state for felids, including *Lynx*.

Lynx affinity of the small cranium from Longdan

The feline cranium HMV2010 from Longdan has characteristic *Lynx* craniodental

features. The cranium is relatively broad, and the upper canine has two deep buccal grooves, and one distinct anterior groove. The P2 is absent. This trait combination is not seen in any other genera of Felidae. Of noteworthy importance is the feature of the upper canine. As mentioned above, the presence of anterior groove is only present in *Lynx* among the Old World feline, and at least since the Late Pliocene. In the New World, most species of *Leopardus* also have deep buccal grooves and distinct anterior groove, but this genus typically retains P2 (except *Leopardus colocolo*, which frequently lack this tooth), and distinctly lower zygomatic arch, so the Longdan felid is unlikely a member of *Leopardus*.

The Longdan *Lynx* is also different from all living and known fossil species of *Lynx*. The body size of Longdan *Lynx* is distinctly smaller than that of *L. issiodorensis* from the same locality and other eastern Asian records (e.g., Yushe Basin, Nihewan Basin) and is also smaller than all living species except *L. rufus* (Fig. 8). The general morphology is similar to that of *L. rufus*, e.g., relatively narrow rostrum, P4 parastyle not elongated. However, The Longdan *Lynx* has a wider zygomatic width, and deeper zygomatic arch than those of *L. rufus*. The other three living species of *Lynx* have broader cranium and more elongated P4 parastyle. In Europe, the early and middle Villafranchian lynx generally has a large body size, but since the late Villafranchian or slightly earlier, some smaller-sized population appeared (Mecozzi et al., 2021; Cuccu et al., 2022). The Longdan felid is still distinctly smaller than these lynx population (P4 of the small individual of late Villafranchian *L. issiodorensis* is still larger than 17 mm) (Werdelin, 1981). *L. issiodorensis* from Longdan shows clear affinity to *L. lynx* in size, dental robustness (Fig. 8A-B), but also differs significantly in relatively P3 size (Fig. 8-E), rostrum length and width (Fig. 8G-I). A more detailed analysis of different

populations of *L. issiodorensis* and their comparison with the living species will be the topic for future more specific works. Both the type of *L. issiodorensis* and the Longdan population of this species are distinctly larger than *L. hei* in all lineal measurements, and has larger postorbital process of the frontal, but the craniodental proportions of the two species are similar. The type of *L. issiodorensis* also has a deeper zygomatic arch and proportionally smaller auditory bulla. *L. canadensis* is only slightly larger than *L. rufus*, but it differs significantly from the latter in several aspects, e.g., narrower cheek teeth, distinctly longer P4 parastyle and wider rostrum. The Longdan felid is therefore represents a new species of *Lynx*, i.e., *L. hei* sp. nov.

The diversification of *Lynx* during the Plio-Pleistocene

To better study the phylogenetic position of *L. hei*, and the diversification of *Lynx* during the Plio-Pleistocene, we performed phylogenetic analyses for all living species of *Lynx*, *L. issiodorensis*, *L. hei*, and most living genera of Felidae, in fact the first phylogenetic analysis ever performed in fossil lynx. Note that our matrix coding of *L. issiodorensis* is based on materials from Shouyang, Yushe, and Longdan of eastern Asia.

In addition to Maximum Parsimony analysis, we perform Bayes Inference analysis under Mkv model (Lewis, 2001), as it outperforms Maximum Parsimony for estimation of phylogeny from discrete morphological data (Wright and Hillis, 2014), but see some debate in Goloboff et al. (2018). Our morphological matrix is based on matrix of Salles (1992) and Werdelin and Flink (2018), and expanded considerably based on our observation of all living and selected fossil species of Felidae. Those only characteristic of machairodonts (subfamily

Machairodontinae) were not included in the analysis. Apomorphy for each species is retained when available, as it is informative in the tip-dating analysis (Matzke and Irmis, 2018; Zhang and Wang, 2019). The gray wolf *Canis lupus* and the fossa *Cryptoprocta ferox* were chosen as the outgroup for Felidae following the choice of Werdelin and Flink (2018). Two Miocene felids *Proailurus lemanensis* and *Hyperailurictis intrepidus* were chosen to represent the primitive members of the subfamily. The majority of the living genera (here including 11 genera in addition to *Lynx*) were included in the analyses. In Bayes Inference analyses, we performed both ordinary and tip-dating methods (Ronquist et al., 2012a). In the latter method, we did not include molecular data, so the tip-dating mainly acts as a constraint on branch length. As our fossil sampling of fossil feline is insufficient, we did not analyze the divergent time inferred from the tip-dating method, which can be more reliable when more fossil members were included in the analyses.

In two of the three analyses (MP, BI, tip-dating BI), the monophyly of *Lynx* is not supported, and *Otocolobus manul* mostly groups within *Lynx*. Even though molecular phylogeny clearly suggested that *O. manul* has a closer relationship to *Prionailurus* (Johnson et al., 2006; Li et al., 2016), our result is expected from a morphological aspect, as there is considerable convergence. *O. manul* has a broad cranium, wide forehead, absence of the P2, and reduction of the P4 protocone, elongated m1, that are also present in three living species of *Lynx* (not in *L. rufus*). In BI analysis, *Acinonyx jubatus* groups into *Lynx*, as there is also convergence between them, e.g., p4 anterior accessory cuspid enlarged, deep mandibular corpus. In MP analysis, the two species of *Panthera* are grouped with *Acinonyx*, together in *Lynx*, in a similar result of convergence. In the final analyses, we use constraint forcing

Otocolobus grouped with *Prionailurus*, and *Acinonyx* grouped with *Puma*, as we regard that molecular lineage defined by Johnson et al. (2006) as correct, considering its data size.

Nevertheless, all Bayes analyses (Fig. 9 and appendix), *L. hei* and *L. issiodorensis* are grouped within the crown group of *Lynx*. In MP analysis, *L. issiodorensis* is grouped with *L. lynx*, *L. pardinus* and *L. canadensis*, whereas the position of *L. hei* is not resolved in the strict consensus tree. We checked the original equal parsimony tree and found that this species is either sister to *L. rufus*, or sister to the group of *L. issiodorensis* + three living species of *Lynx*. In the BI analyses after constraining *Otocolobus* and *Acinonyx* out of *Lynx*, both tip-dating and ordinary analyses support the sister group *L. hei* and *L. rufus*, and *L. issiodorensis* to the other three species of *Lynx*, but in ordinary BI analysis, the posterior probability for the internal node within *Lynx* is rather low. In the tip-dating BI analysis without constraint, *L. issiodorensis* is grouped with *L. hei* + *L. rufus*, but with rather low posterior probability for this node. In most analyses (e.g., ordinary BI and MP analyses without constraint), the Asiatic golden cat *Catopuma* is supported as a sister group to *Lynx*. This result is congruent with the recent genomic phylogeny (Li et al., 2016). Another relationship of the recent genomic phylogeny, which *Felis* and *Prionailurus* are sister groups, is also supported in our analyses. Some other relationship, e.g., the sister group of *Puma* and *Acinonyx*, is not supported in any non-constraint analyses. This result is likely due to the lacking in intermedium form between the much more specialized *Acinonyx* and more conservative *Puma*, leaving a considerable morphological gap between them. Adding more fossil members will be helpful to break this long branch.

Our analyses provide interesting new information on the diversification of the crown

members of *Lynx*. The fossil records of *Lynx* are quite common in Eurasia, but mostly assigned to *L. issiodorensis*, which was supposed to be the common ancestor for the three other living species of *Lynx*, suggesting a simple widely distributed common ancestor-vicariance-speciation model. Our new finding suggested that *Lynx* crown group already experienced diversification during the Plio-Pleistocene. Molecular phylogenetic dating (Li et al., 2016) suggests a middle Pliocene divergence bobcat *L. rufus* to the rest of living species. Our new fossil and phylogeny support such a scenario. *Lynx* began to diverge into two ecomorphologically different species during the middle Pliocene, differs mainly by their body size. One population of the small-sized lineage migrated to North America and evolved there since then, finally evolved to the living *L. rufus*, whereas *L. hei* represents the population of this small-sized lineage retained in eastern Asia. At this evolutionary level, both large and small-sized lineage still have primitive craniodental traits, e.g., skull relatively narrow, and cheek teeth not enlarged. These traits are retained in *L. rufus*, whereas *L. issiodorensis* experienced to the second wave of diversification since the Pleistocene, and acquired more derived traits, e.g., broad skull, shorter rostrum.

It is interesting to note that after the larger sized lineage acquirement of a broad skull, shorter rostrum, it then began to occupy the niche of smaller body size: living *L. canadensis* has a comparative body size similar to *L. rufus*. This pattern suggests the first divergence of ecomorphology is achieved by evolving into different body size, and during the evolutionary history, the two lineages gradually their unique morphology, large enough to allow them to explore different niches without body size differences, as is seen in the living *L. canadensis* and *L. rufus* (Fig. 10).

Conclusion

The new Early Pleistocene fossil cranium from Longdan described here, represents a new species of lynx, *L. hei*, phylogenetically closely related to the modern North American *L. rufus*. Our phylogeny and comparative analyses suggest that the crown group of *Lynx* experienced its initial diversification during the mid-Pliocene in Eurasia into two lineages i.e., *L. hei-rufus*, and *L. issiodorensis*-other living species. The two lineages mainly differ in their body size during the Plio-Pleistocene. Whereas latter larger sized lineage acquired new craniodental morphology, and experienced a second wave of diversification in radiation in body size/morphology during the Pleistocene.

Acknowledgements: We thank J. Meng, R. O'Leary, and J. Galkin for their help in accessing the AMNH fossil mammal collections; M. Surovy, E. Hoeger, and S. Ketelsen for their help in accessing the AMNH modern mammal collections; A. Millhouse, D. Lunde and J. J. Ososky for their help in accessing the USNM fossil and modern mammal collections; and Z. Qiu and J. Chen, W. He, S. Chen for help in accessing fossil collections of the IVPP and HMV. The current work was supported by the Strategic Priority Research Program of Chinese Academy of Sciences (Grant No. XDB26000000 and XDA20070203), Key Frontier Science Research Program of the Chinese Academy of Sciences (Grant Nos. QYZDY-SSW-DQC-22 and GJHZ1885), the National Natural Science Foundation of China (Grant Nos. 42102001, 41430102, 41872001, 41872005 and 41772018), Second Comprehensive Scientific Expedition on the Tibetan Plateau [2019QZKK0705], China Scholarship Council, and Frick Fund, Division of Vertebrate Paleontology, AMNH. J.M.-M. was funded by the

Agencia Estatal de Investigación-European Regional Development Fund of the European Union (CGL2017-82654-P, AEI/FEDER-UE) and the Generalitat de Catalunya (CERCA Program). J.M.-M. is member of the consolidated research group 2017 SGR 116 (AGAUR, Generalitat de Catalunya).

References

Batsch, A.J.G.C., 1788. Versuch einer Anleitung, zur Kenntniβ und Geschichte der Thiere und Mineralien, für akademische Vorlesungen entworfen und mit den nöthigsten Abbildungen versehen Erster Theil. Academischen Buchhandlung, Jena.

Bellani, G.G., 2019. Felines of the World: Discoveries in Taxonomic Classification and History. Academic Press, London.

Boscaini, A., Alba, D.M., Beltrán, J.F., Moyà-Solà, S., Madurell-Malapeira, J., 2016. Latest Early Pleistocene remains of Lynx pardinus (Carnivora, Felidae) from the Iberian Peninsula: taxonomy and evolutionary implications. Quaternary Science Reviews 143, 96-106.

Bowdich, T.E., 1821. An Analysis of the Natural Classification of Mammalia, for Use of Students and Travelers. J. Smith, Paris.

Chamberlain, M.J., Leopold, B.D., Conner, L.M., 2003. Space use, movements and habitat selection of adult bobcats (*Lynx rufus*) in central Mississippi. The American Midland Naturalist 149, 395-405.

Croizet, J.B., Jobert, A.C.G., 1828. Recherches sur les ossemens fossiles du département du Puy-de-Dôme. Paris: Chez les principaux libraires, 1-224.

Cuccu, A., Valenciano, A., Azanza, B., DeMiguel, D., 2022. A new lynx mandible from the Early Pleistocene of Spain (La Puebla de Valverde, Teruel) and a taxonomical multivariate approach of medium-sized felids. Historical Biology, 1-12.

Geraads, D., 1980. Un nouveau felide (Fissipeda, mammalia) du pleistocene moyen du Maroc: Lynx thomasi N. sp. Geobios 13, 441-444.

Geraads, D., 2016. Pleistocene Carnivora (Mammalia) from Tighennif (Ternifine), Algeria. Geobios 49, 445–458.

Goloboff, P.A., Catalano, S.A., 2016. TNT version 1.5, including a full implementation of phylogenetic morphometrics. Cladistics 32, 221-238.

Goloboff, P.A., Farris, J.S., Nixon, K.C., 2008. TNT, a free program for phylogenetic analysis. Cladistics 24, 774-786.

Goloboff, P.A., Torres, A., Arias, J.S., 2018. Weighted parsimony outperforms other methods of phylogenetic inference under models appropriate for morphology. Cladistics 34, 407-437.

Hendey, Q.B., 1974. The Late Cenozoic Carnivora of the Southwestern Cape Province South Africa. Annals of the South African Museum 63, 1-369.

Heptner, V.G., 1992. Mammals of the Soviet Union, Volume 2 Part 2 Carnivora (Hyenas and Cats). Brill.

Huelsenbeck, J.P., Ronquist, F., 2001. MRBAYES: Bayesian inference of phylogenetic trees. Bioinformatics 17, 754-755.

Jayne, H., 1898. Mammalian Anatomy, Part I. The Skeleton of the Cat. Lippincott Company, London.

406 Johnson, W.E., Eizirik, E., Pecon-Slattery, J., Murphy, W.J., Antunes, A., Teeling, E., O'Brien, S.J., 2006. The late
407 Miocene radiation of modern Felidae: a genetic assessment. Science 311, 73-77.
408 Kerr, R., 1792. The animal kingdom or zoological system, of the celebrated Sir Charles Linnaeus…, London.
409 Kurtén, B., Werdelin, L., 1984. The relationships of *Lynx shansius* Teilhard. Annales Zoologici Fennici, 129-133.
410 Lewis, P.O., 2001. A likelihood approach to estimating phylogeny from discrete morphological character data.
411 Syst Biol 50, 913-925.
412 Li, G., Davis, B.W., Eizirik, E., Murphy, W.J., 2016. Phylogenomic evidence for ancient hybridization in the
413 genomes of living cats (Felidae). Genome Res 26, 1-11.
414 Lovallo, M.J., Anderson, E.M., 1996. Bobcat (*Lynx rufus*) home range size and habitat use in northwest Wisconsin.
415 American Midland Naturalist, 241-252.
416 Maddison, D.R., Maddison, W.P., 2021. Mesquite: a modular system for evolutionary analysis. Version 3.40
417 https://www.mesquiteproject.org/home.html.
418 Matzke, N.J., Irmis, R.B., 2018. Including autapomorphies is important for paleontological tip-dating with
419 clocklike data, but not with non-clock data. PeerJ 6, e4553.
420 Mecozzi, B., Sardella, R., Boscaini, A., Cherin, M., Costeur, L., Madurell-Malapeira, J., Pavia, M., Profico, A.,
421 Iurino, D.A., 2021. The tale of a short-tailed cat: New outstanding Late Pleistocene fossils of Lynx
422 pardinus from southern Italy. Quaternary Science Reviews 262, 106840.
423 Poole, K.G., 2003. A review of the Canada lynx, *Lynx canadensis*, in Canada. The Canadian Field-Naturalist 117,
424 360-376.
425 Qiu, Z.X., Deng, T., Wang, B.Y., 2004. Early pleistocene mammalian fauna from Longdan, Dongxiang, Gansu,
426 China. Science Press, Beijing.
427 Qiu, Z.X., Deng, T., Wang, B.Y., 2014. A Late Miocene *Ursavus* skull from Guanghe, Gansu, China. Vertebrata
428 PalAsiatica 52, 265-302.
429 Ronquist, F., Klopfstein, S., Vilhelmsen, L., Schulmeister, S., Murray, D.L., Rasnitsyn, A.P., 2012a. A total-
430 evidence approach to dating with fossils, applied to the early radiation of the hymenoptera. Syst Biol 61,
431 973-999.
432 Ronquist, F., Teslenko, M., van der Mark, P., Ayres, D.L., Darling, A., Hohna, S., Larget, B., Liu, L., Suchard,
433 M.A., Huelsenbeck, J.P., 2012b. MrBayes 3.2: efficient Bayesian phylogenetic inference and model
434 choice across a large model space. Syst Biol 61, 539-542.
435 Salles, L.O., 1992. Felid phylogenetics: extant taxa and skull morphology (Felidae, Aeluroidea). American
436 Museum Novitates 3047, 1-67.
437 Schultz, C.B., Martin, L.D., 1972. Two lynx-like cats from the Pliocene and Pleistocene. Buletin of the University
438 of Nebraska State Museum 9, 197-203.
439 Sunquist, M., Sunquist, F., 2002. Wild cats of the world. University of Chicago press, Chicago.
440 Teilhard de Chardin, P., Leroy, P., 1945. Les Felides de Chine. Institut de géobiologie, Pekin.
441 Tumlison, R., 1987. *Felis lynx*. Mammalian species 269, 1-8.
442 Werdelin, L., 1981. The evolution of lynxes, Annales Zoologici Fennici. JSTOR, pp. 37-71.
443 Werdelin, L., Flink, T., 2018. The phylogenetic context of Smilodon, in: Werdelin, L., Mcdonald, H.G., Shaw,
444 C.A. (Eds.), Smilodon: The Iconic Sabertooth. Johns Hopkins University Press, Baltimore, pp. 14-29.
445 Wright, A.M., Hillis, D.M., 2014. Bayesian Analysis Using a Simple Likelihood Model Outperforms Parsimony
446 for Estimation of Phylogeny from Discrete Morphological Data. PloS one 9, e109210.
447 Zhang, C., Wang, M., 2019. Bayesian tip dating reveals heterogeneous morphological clocks in Mesozoic birds.
448 R Soc Open Sci 6, 182062.

449

Figure captions

Fig. 1. Location of Longdan.

Fig. 2. Craniodental measurement of *Lynx* used in this study. For measurements see Abbreviation section.

Fig. 3. Holotype of *Lynx hei* sp. nov, HMV2010, from Longdan.

Fig. 4. Anterior view of rostrum of various *Lynx* species, marking the presence of the anterior groove in the upper canine. A. *L. hei* sp. nov., HMV2010; B. *L. issiodorensis*, HMV2015; C. *L. canadensis*, USNM212620; D. *L. rufus*, AMNH 24666. Not to scale.

Fig. 5. Comparison of occlusal view of upper cheek tooth rows of *Lynx* spp.. A. *L. issiodorensis*, A1. HMV2012, Longdan; A2. AMNH 96-B1042 (reversed/mirrored), Xiazhuang, and A3. AMNH 62-B756, both Shouyang; B. *L. hei* sp. nov., HMV2010, Longdan; C. *L. rufus*, C1. AMNH M14822; C2. AMNH M243108; D. *L. pardinus*, D1. AMNH M169492; D2. USNM 152619; E. *L. canadensis*, E1. USNM 077095; E2. USNM 212617; F. *L. lynx*, F1. AMNH 41337; F2. IOZ T0139.

Fig. 6. Comparison of buccal view of *Lynx* spp. A. *Lynx canadensis*, USNM 025726; B. *L. rufus*, USNM 243108; C. *L. hei* sp. nov., HMV 2010; D. *L. issiodorensis*, ; E. *L. issiodorensis*, Longdan, HMV2016; F. *L. issiodorensis*, Xiazhuang, Shouyang, AMNH 96-B,1024. Not to scale.

Fig. 7. Crania of *Lynx hei*, and selected living felid species, lateral, ventral and dorsal views. A. *L. hei*, HMV2010; B. *L. rufus*, AMNH M24665; C. *L. candaensis*, USNM33126; D. *L. pardinus*, AMNH M169492; E. *L. lynx*, IOZ09419, F. *Caracal caracal*, AMNH

M116512.

Fig. 8. Craniodental measurements and ratio of *Lynx hei* sp. nov. and related taxa. A. P3 length vs width/length ratio; B. P4 length vs width/length ratio; C. P4 length vs blade width/length ratio; D. P4 length vs parastyle length/length ratio; E. P4 length vs P3/P4 length ratio; F. condylobasal length vs toothrow length; G. toothrow length vs diastema/toothrow length ratio; H. condylobasal length vs rostrum width cross P4 and m1/condylobasal length ratio; I. condylobasal length vs rostrum width cross C/condylobasal length ratio.

Fig. 9. Bayes Inference tip-dating analysis, with constraint on *Otocolobus* with *Prionailurus*. See the results of other phylogenies in appendix.

Fig. 10. Model of diversification pattern of *Lynx* proposed in this paper. The specimen of *L. issiodorensis* HMV2015 is from Longdan, China.


Longdan

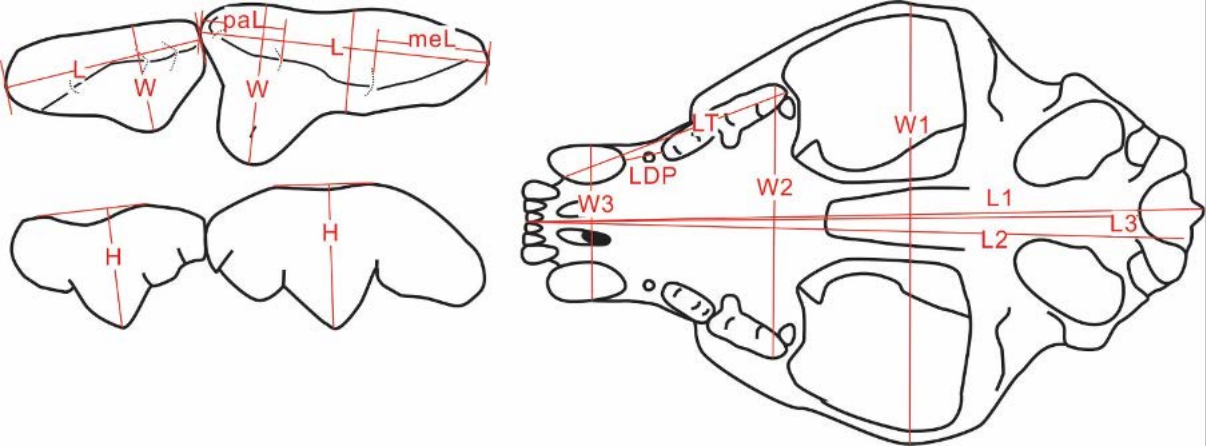
paL
L
meL
L
W
W
H
H
LT
W1
LDP
W2
W3
L1
L3
L2

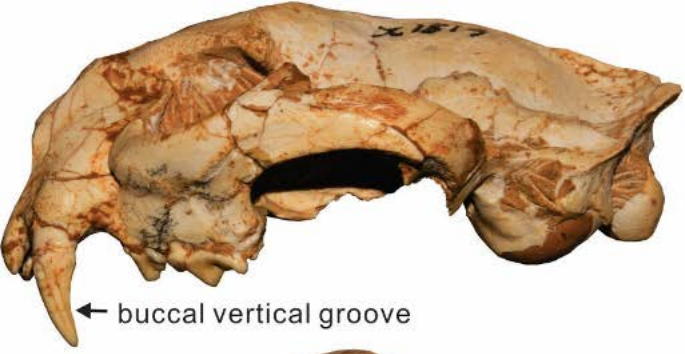
buccal vertical groove


anterior vertical groove


X1813

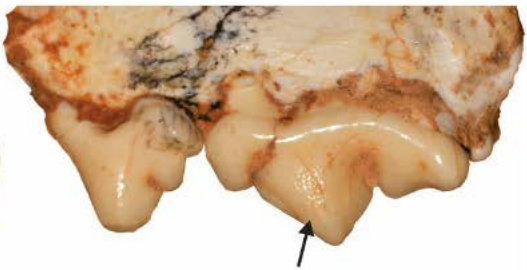
no buccal vertical groove


A
B
C
D

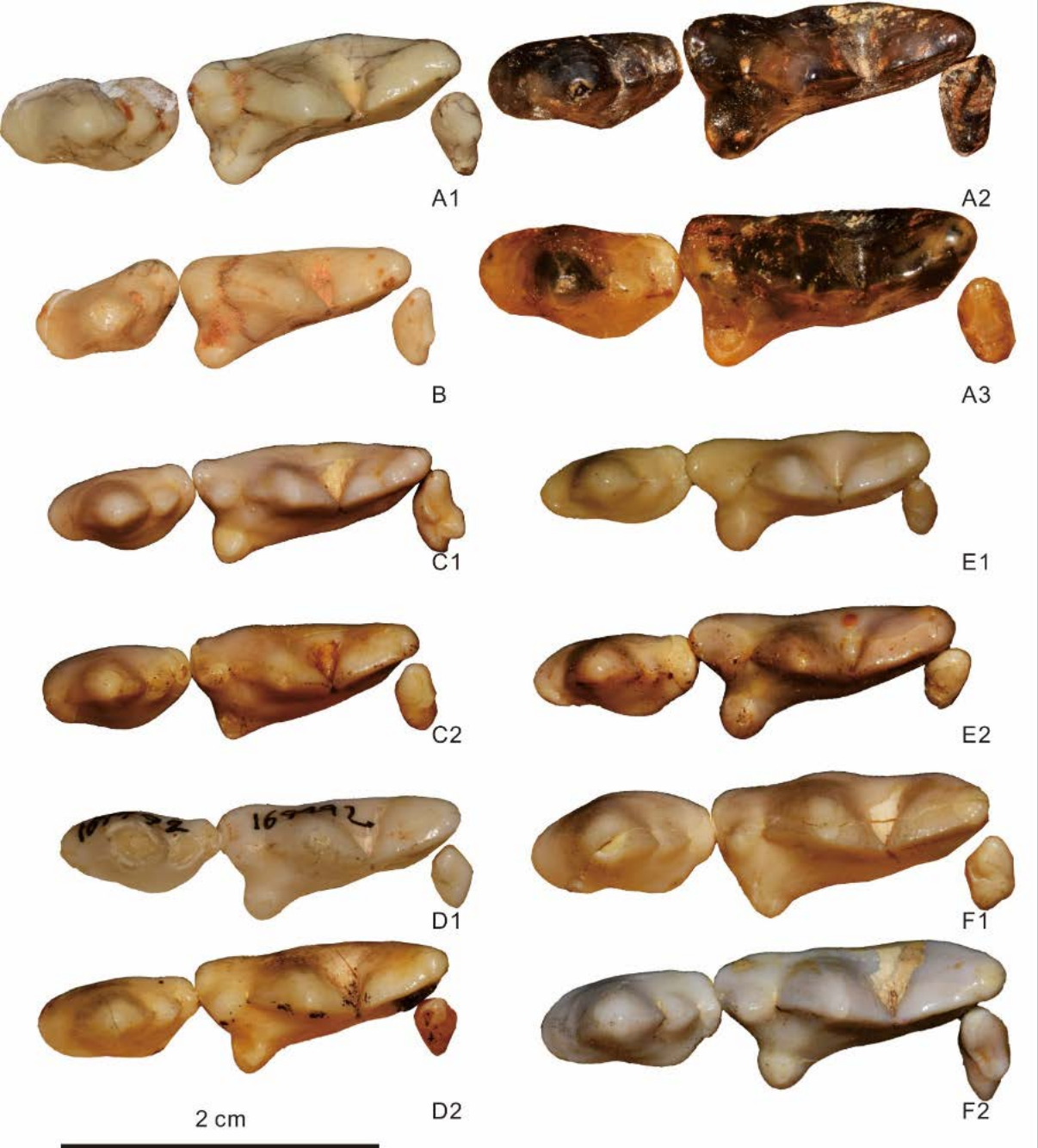
A1
A2
B
A3
C1
E1
C2
E2
D1
F1
D2
F2
2 cm

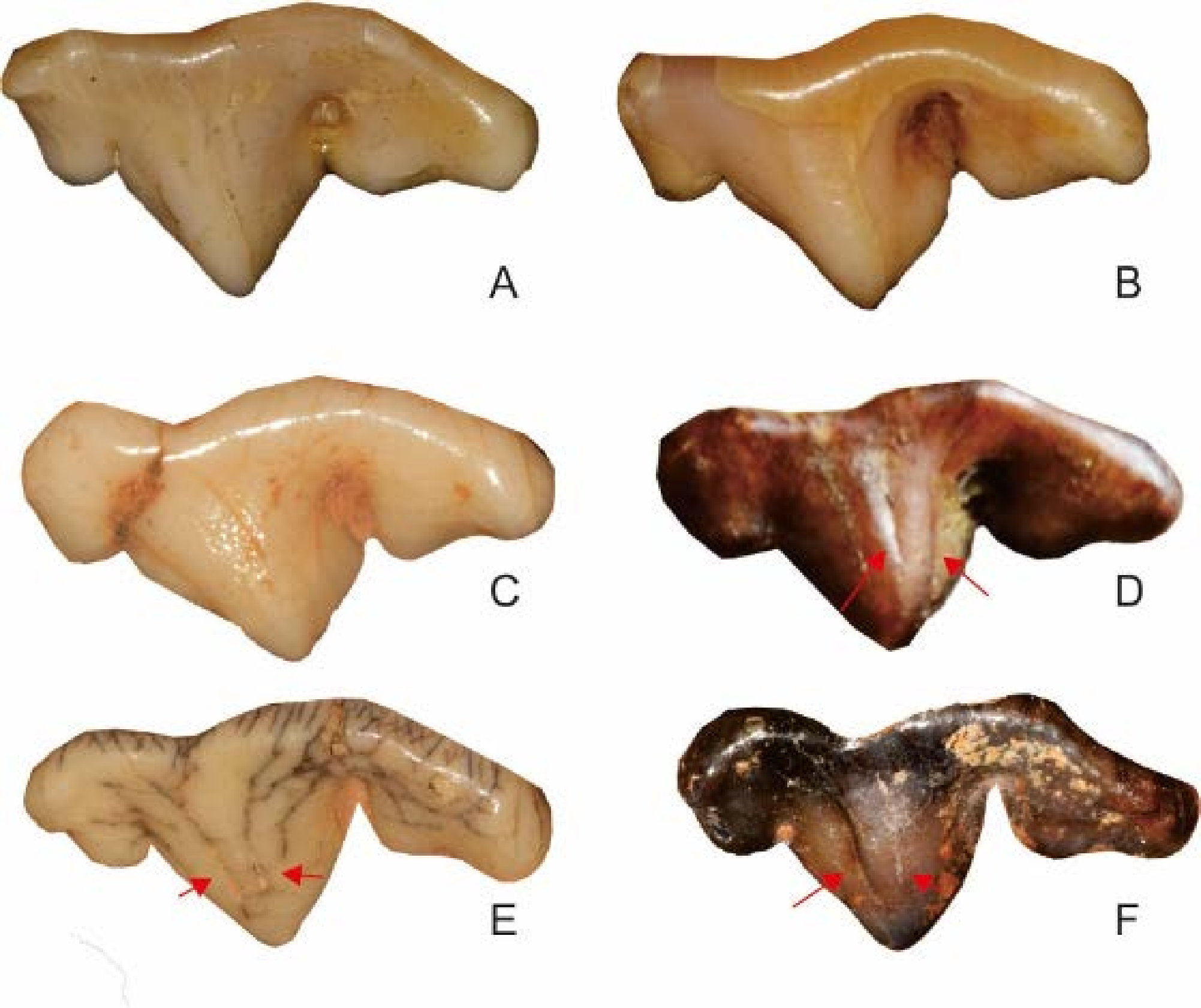
A
B
C
D
E
F

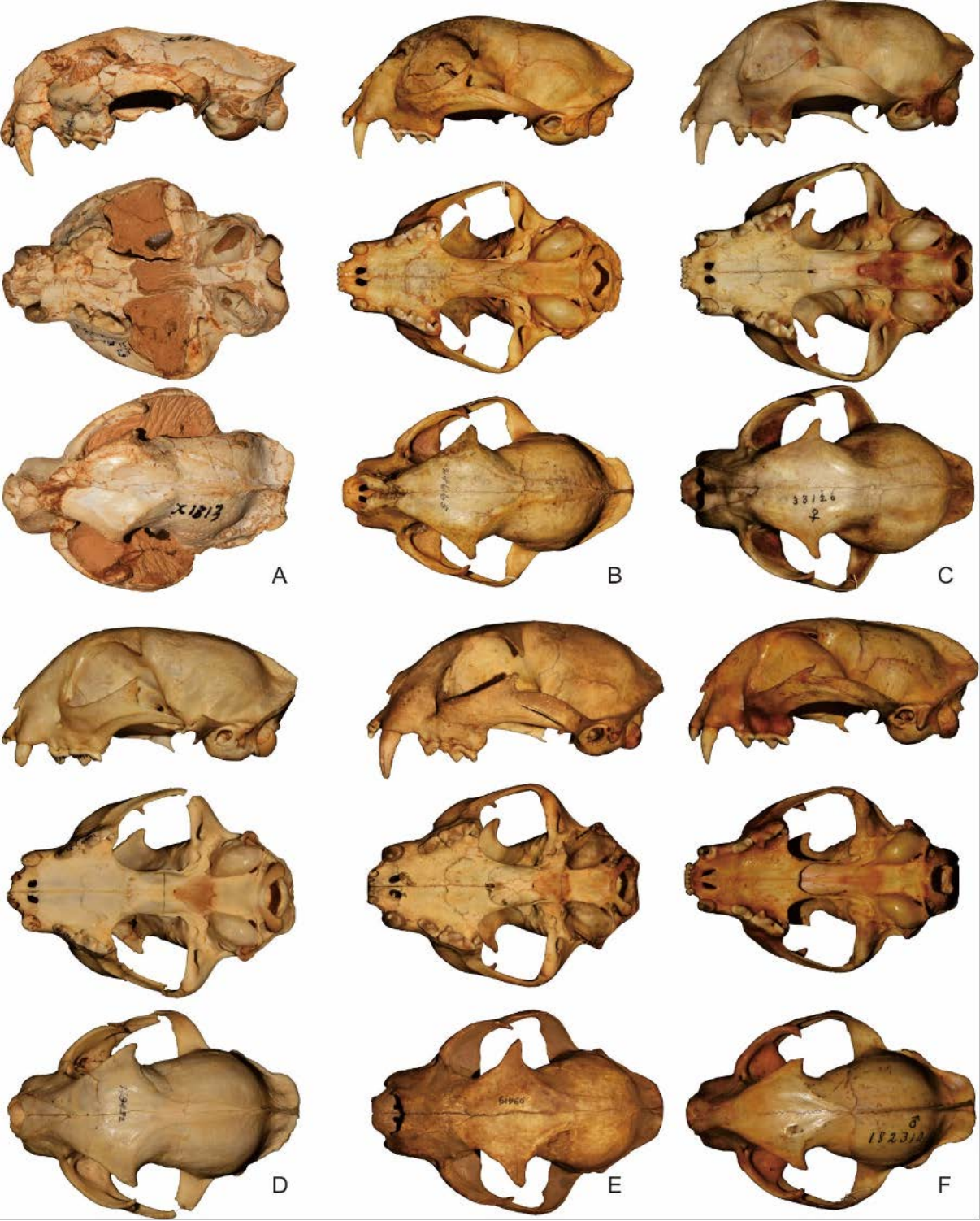
X1813
A
B
33126
♀
C
D
E
♂
F

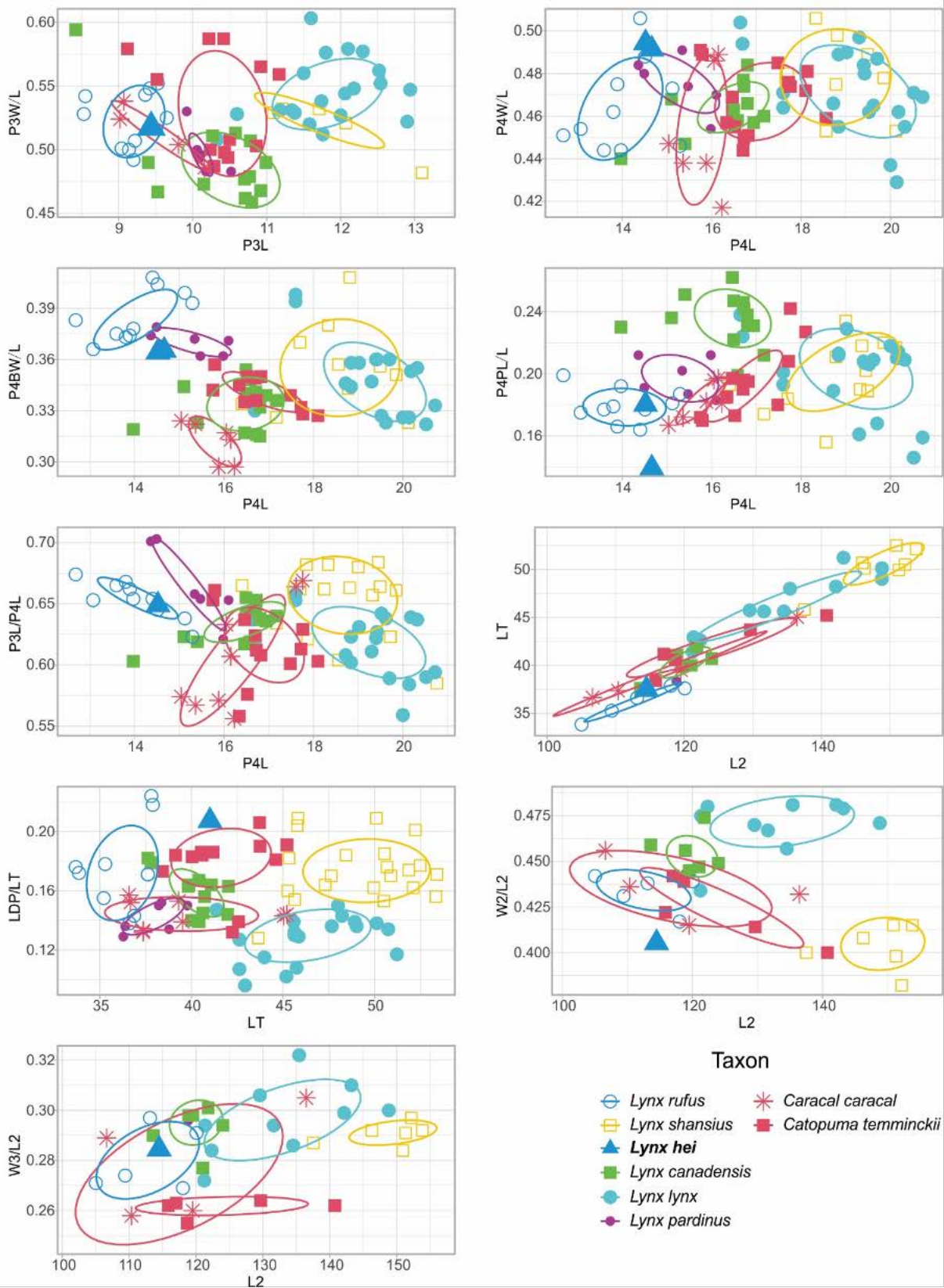
P3W/L
P3L
P4W/L
P4L
P4BW/L
P4L
P4PL/L
P4L
P3L/P4L
P4L
LT
L2
LDP/LT
LT
W2/L2
L2
W3/L2
L2
Taxon
Lynx rufus
Lynx shansius
Lynx hei
Lynx canadensis
Lynx lynx
Lynx pardinus
Caracal caracal
Catopuma temminckii

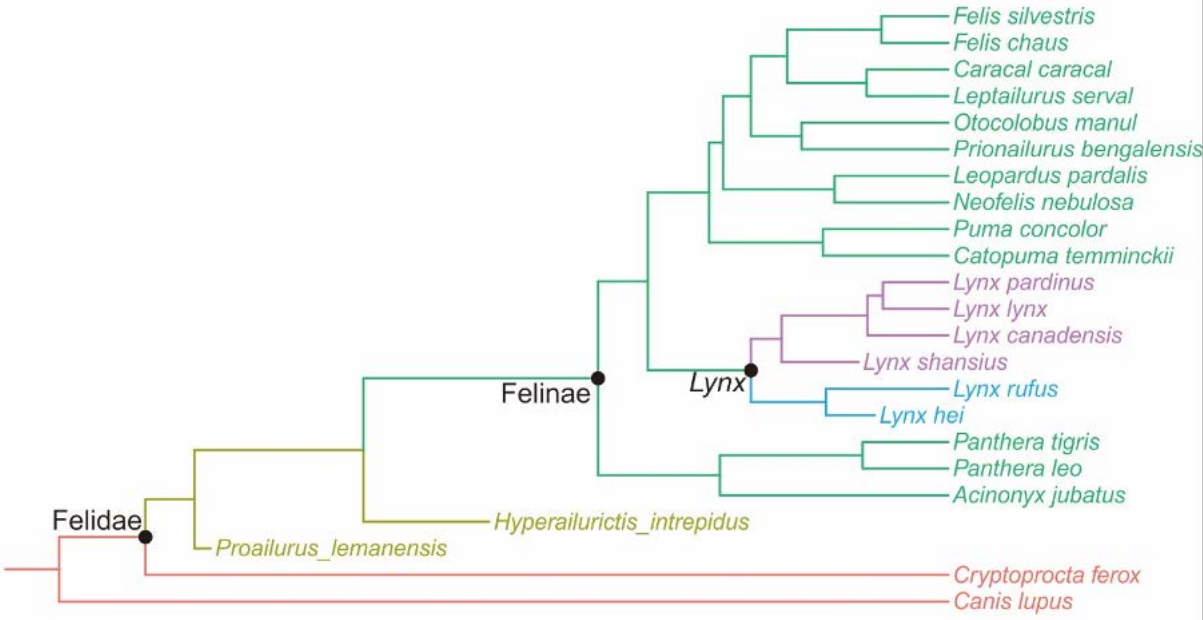
Felis silvestris
Felis chaus
Caracal caracal
Leptailurus serval
Otocolobus manul
Prionailurus bengalensis
Leopardus pardalis
Neofelis nebulosa
Puma concolor
Catopuma temminckii
Lynx pardinus
Lynx lynx
Lynx canadensis
Lynx shansius
Lynx rufus
Lynx hei
Panthera tigris
Panthera leo
Acinonyx jubatus
Felinae
Lynx
Felidae
Hyperailurictis_intrepidus
Proailurus_lemanensis
Cryptoprocta ferox
Canis lupus

1993	old No.	No.	note		Character	0	1	2	3	
		1		canine	Upper canine morphology height	reduced (<0.13)	crown not elongated (~13–20% of c	moderately elongate (~20–25%)	25-35	(>35% of CBL)
		2		canine	Upper canine buccal groove	0	1	2	3	
		3		canine	Upper canine lingual groove	0	1	2		
		4		canine	Lower canine buccal groove	0	1	2		
	4	5		canine	lower canine morphology	caniniform and large	small	very small and incisiform		
		6		M1	M1 transverelg shortening	not shortened (>2)	shortened (<2)			
		7		M1	M1 cusp	presence of large, multicuspid M1 si	presence of reduced, multi-cuspid M	no distinct cusp		
	7	8		P4	P4 protocone morphology	presence of large, usually cusped pr	protocone small but still distinct	protocone very small or absent		
	8	9		P4	P4 protocone angulation	P4 protocone angulation	strongly anteriorly directed	lingually directed		
	9	10		P4	P4 protocone position	anterior to the paracone-parastyle ju	at the paracone-parastyle junction	posterior to the paracone-parastyle junction		
	10	11		P4	P4 parastyle anteroposterior length	absent or cingulum-like	small (<0.2)	moderate (0.2-0.25)	large (>0.25)	
		12		P4	P4 buccal concavity	absent	one	two		
	11	13		P4	P4 preparastyle size	absent	small	large		
		14		P4	P4 preparastyle direction	nearly perpendicular to parastyle	with distinct angle with parastyle	nearly in line with parastyle		
		15		P4	P4 buccal vertical groove	absent	present			
	12	16		P4	Relative size of P4	P4 short relative to PL (<25% of PL	P4 long relative to PL (>25% of PL)			
	13	17		P3	Relative length P3/P4	P3 long relative to P4 (>60% of LP4	P3 moderate (ca. 50–60% of LP4)	P3 short (ca. 35–50% of LP4)	P3 very short (<35% of LP4)	
	14	18		P3	P3 posterior cingulum	absent or weak	distinct	cusp-like		
	15	19		P3	P3 anterior accessory cusp	absent	present	large		
		20		P3	P3 anterior cingulid cusp	absent	often present			
		21		P3	anterior end of P3 anterior ridge	close to the anterior border	distinctly lingually			
9		22		P3	P3 lingual ridge	absent	present			
	16	23		P3	Greatest width of P3	at main cusp	posterior part	distal part		
	17	24		P2	P2 morphology	large with multiple cusps	present but very small, usually only	absent		
		25		P2	P2 root	double	single			
	18	26		P1	P1 morphology	present	present but very small	absent		
	19	27		m3	m3 presence	Present	absent			
	20	28		m2	m2 presence	Present	absent			
	21	29		m1	m1 metaconid-talonid morphology	large talonid basin with distinct hypc	large without basin	small	absent	
		30		m1	m1 metaconid and talonid differential	differential	undistinguishable			
		31		m1	m1 widest part	posterior to the paraconid-protoconi	at the paraconid-protoconid notch	slightly anterior to the paraconid-pro	near the middle part of the paraconid	
		32		m1	m1 robustness (W/L)	slender (mostly <45%)	robust (~50%)			
		33		m1	anterior border	vertical or slightly posteriorly incline	distinctly posteriorly inclined			
	24	34		m1	Relative size of m1	short relative to mandible length (<1	long relative to mandible length (>15%)			
	22	35		p4	p4 relative length	long (>80% of m1 length)	short (<80% of m1 length)			
	25	36		p4	p4 paraconid direction	posterior inclined	vertical			
		37		p4	p4 paraconid size	distinctly smaller than the posterior a	similar to the posterior accessory cu	larger than the posterior accessory cuspid		
		38		p4	p4 posterior cingulid	absent or weak	clearly distinguished	cusp-like		
		39		p4	middle constriction	generally absent	generally present			
	47	40		p3	p3 size (versus m1)	small (<0.3%) or absent	relatively small (0.3-0.5)	large		
		41		p3	p3 height	same or slightly lower than the p4 (>	distinctly lower than the p4 (<0.7)			
		42		p3	p3 anterior accessory cusp	absent	indistinct	distinct		
		43		p3	p3 posterior cingulid	absent or weak	clearly distinguished	cusp-like		
	26	44		p2	p2 presence	Present	absent			
	27	45		p1	p1 presence	Present	absent			
		46		cranium	dorsal concavity between C-P4	absent	present			
		47		cranium	zygomatic arch deepth	narrow	deep			
	31	48		cranium	Anterior border of orbit	at anterior border of P3	P3	P3/P4 to P4 paracone	P4 metacone	
	34	49		cranium	Infraorbital fenestra position	at anterior border of P3	P3	at around P3/P4	posterior to P3/P4	
		50		cranium	Infraorbital fenestra size	very small (Acinonyx)	small (Felis)	large (Panthera)	very large (Smilodon)	
	32	51		cranium	Snout area elevation compared with braincase	snout area low	snout area distinctly elevated			
		52		cranium	cranial dorsal contour	nearly straight	with distinct angle	rounded		
		53		cranium	forehead width	distinctly wider than the rostrum	similar to the rostrum			
	35	54		cranium	extension of posterior border of the nasals relative to maxi	not extended	similar	more extended		
	45	55		cranium	posterior arch nasals	weakly arched	arched			
		56		cranium	posterior border shape of the nasals	smooth	pointed			
		57		cranium	anterior process of frontal	weak	strong			
		58		cranium	nasal width	narrow	wide			
37		59		cranium	nasal middle constriction (Rostral constriction)	absent	present			
38		60		cranium	Nasal curvature	absent	present			
		61		cranium	depression at the posterior end of nasal	absent	present			
31		62		cranium	Frontal bone, outer surface depression	absent	present			
43		63		cranium	anterior border of jugal	strongly anteriorly inclined	moderately anteriorly inclined			
44		64		cranium	Lower rim of the orbit	vertical	flat			
	36	65		cranium	Size of the jugal postorbital process	small, rounded, often almost absent	rounded triangle	long, pointed		
	37	66		cranium	Angle of the occipital condyles	low (~45–60)	high (~70–100)			
	38	67		cranium	rostrum width vs palatine width	narrow, <0.7	wide 0.7-0.8	very wide >0.8		
	39	68		cranium	palatine width versus CBL	widest part of the palate comparative	widest part of the palate comparative	widest part of the palate comparatively narrow wide (>45%)		
	40	69		cranium	Alisphenoid canal	Present	absent			
		70		cranium	occipital condyle position	low, much lower than the middle po	high, close to the middle point of inion and mastoid process			
	46	71		cranium	Orientation of P3 and P4	tiny angle or nearly in line	small angle	large angle		
		72		cranium	extension of bony choana	at or slightly posterior to the M1	distinctly posterior to the M1			
		73		cranium	palate concavity medial to the M1	absent or weak	distinct			
		74		cranium	position of rounded foramen	very close to the orbital fissure	at the middle of orbital fissure and oval foramen			
		75		cranium	pterygoid fossa	absent	small	distinct		
		76		cranium	middle ear opening	moderate	enlarged			
		77		cranium	sagittal crest	always present	often or always absent			
		78		cranium	postorbital bar	absent	often present			
		79		cranium	size of ectotympanic	distinctly smaller than the entotympa	enlarged to similar size of ectotympanic			
		80		cranium	anterior projection of jugal	absent	present			
		81		cranium	postorbital constriction	absent or indistinct	distinct			
		82		cranium	posterior expansion of frontal	absent or very weak	distinct			
		83		mandible	number of mental foramina	mostly double	mostly single			
		84		mandible	mandible height at canine	very low < 0.9	moderate (0.9-1.1)	high (1.1-1.3)	very high (>1.3)	
		85		mandible	lower border profile	nearly straight	distinctly convex			
	43	86		mandible	Mandibular fossa termination	posterior to the carnassial	well anterior of the posterior edge of the carnassial, frequently terminating around carnassial saddle or even at the m1/p4 junction			
	44	87		mandible	Posterior part of horizontal dentary ramus height relative t	slender (~15–19%)	robust (~20–23%)	very robust >0.23		

catalogue	Locality	Age	taxa	CL	CW	CH	CW/L	CH/L	P3L	P3W	P3H	P3W/L	P3H/L	P4L	P4W	P4BW	P4PaL
HMV 2010 X1813	Longdan	Early Pleisto	Lynx hei	7,7	5,57	17,68	0,723	2,296	9,44	4,9		0,519		14,52	7,19	5,3	2,63
HMV 2010 X1813	Longdan	Early Pleisto	Lynx hei	7,71	6,15	17,31	0,798	2,245						14,66	7,21	5,36	2,05
V13539	Longdan	Early Pleisto	Lynx shansius						13,23		10,11		0,764	20,12	9,12	6,5	4,37
V13539	Longdan	Early Pleisto	Lynx shansius						13,1	6,31	11,04	0,482	0,843				
V13540	Longdan	Early Pleisto	Lynx shansius						12,07	6,29	9,57	0,521	0,793				
V13540	Longdan	Early Pleisto	Lynx shansius	9,28	7,43	20,78	0,801	2,239						18,78	8,92	6,44	3,97
HMV2013 X1799	Longdan	Early Pleisto	Lynx shansius	9,97	8,42		0,845		11,71	6,23	9,29	0,532	0,793	17,7	8,49	6,55	3,25
HMV2013 X1799	Longdan	Early Pleisto	Lynx shansius	9,23	8,32		0,901		11,09	5,87	9,65	0,529	0,87				
HMV2016 X2126	Longdan	Early Pleisto	Lynx shansius	10,38					12,7					19,32			3,67
HMV2016 X2126	Longdan	Early Pleisto	Lynx shansius	10,31					13,3					19,45			3,93
HMV2015 X1849	Longdan	Early Pleisto	Lynx shansius	9,62		23,47		2,44						19,36			4,22
HMV2015 X1849	Longdan	Early Pleisto	Lynx shansius	9,64		22,19		2,302	12,92					19			4,45
HMV2017 01429	Longdan	Early Pleisto	Lynx shansius	10,52													
HMV2017 01429	Longdan	Early Pleisto	Lynx shansius	10,48					12,29					19,72			
HMV2014 X1821	Shitougou	Early Pleisto	Lynx shansius	9,96					12,14					20,76			
HMV2014 X1821	Shitougou	Early Pleisto	Lynx shansius	9,92										20,46			
HMV 2011 X1775	Longdan	Early Pleisto	Lynx shansius	9,05	6,86		0,758		11,21	5,96		0,532		18,56	8,41	6,63	2,89
HMV 2011 X1775	Longdan	Early Pleisto	Lynx shansius	8,79	7,44	21,79											
HMV 2012 X1781	Longdan	Early Pleisto	Lynx shansius	8,38	6,3				10,88	5,4				17,17		5,6	2,99
HMV 2012 X1781	Longdan	Early Pleisto	Lynx shansius	7,93	6,05				10,9	5				16,4	7,49	5,47	3,17
X1812	Longdan	Early Pleisto	Lynx shansius	9,22	7,14				12,16	5,63				17,84			
X1812	Longdan	Early Pleisto	Lynx shansius						11,1	5,53				17,87			
X1868	Longdan	Early Pleisto	Lynx shansius	11,35	9,9				12,47	6,51	9,62			18,81	9,37	7,68	
X1868	Longdan	Early Pleisto	Lynx shansius						13,02								
X1870	Longdan	Early Pleisto	Lynx shansius	8,96	7,5	20,01			12,51	6,24	10,8			18,33	9,27	6,96	
X1870	Longdan	Early Pleisto	Lynx shansius	8,89	7,1												
HMV1230	Longdan	Early Pleisto	Lynx shansius	10,4					12,07	5,65				18,24			
HMV1230	Longdan	Early Pleisto	Lynx shansius	9,82													
HMV1226	Longdan	Early Pleisto	Lynx shansius	10,44	7,8				12,94	6,29	10,55			19,49	9,53	6,94	3,69
HMV1226	Longdan	Early Pleisto	Lynx shansius	10,8	8,37	24,54			13,12	6,1	10,74			19,85	9,49	6,97	4,37
AMNH M4137	Romania	modern	Lynx lynx	9,2	6,92	20,43	0,752	2,221	11,5	6,44	9,76	0,56	0,849	17,6	8,16	7	3,4
AMNH M4137	Romania	modern	Lynx lynx	9,26	6,95	19,66	0,751	2,123	11,58	6,02	10,26	0,52	0,886	17,6	8,29	6,93	3,54
IOZ08119	辉南	modern	Lynx lynx	10,3	7,6	21,1	0,738	2,049	12,1	7	9,7	0,579	0,802	20,52	9,66	6,6	3
IOZ08119	辉南	modern	Lynx lynx	10,1	7,9		0,782		12,3	7,1	10	0,577	0,813	20,72	9,72	6,9	3,3
IOZ09426	黑龙江密山	modern	Lynx lynx	10	7,5		0,75		11,8	6,8		0,576		19,3	9,6	6,7	3,1
IOZ09426	黑龙江密山	modern	Lynx lynx	9,5	7,5		0,789		11,6	7	9,8	0,603	0,845	19,7	9,6	7,1	3,3
IOZ07809	吉林敦化	modern	Lynx lynx	8,52	7,14	20,54	0,838	2,411	11,18	5,94	10,42	0,531	0,932	20	8,74	6,52	4,36
IOZ07809	吉林敦化	modern	Lynx lynx	8,86	7,16	21	0,808	2,37	11,76	6,02	10,72	0,512	0,912	20,14	8,64	6,56	4,22
IOZ09422	大约是东北	modern	Lynx lynx	10,92	8,92		0,817		12,9	6,74	10,74	0,522	0,833	20,18	9,32	7,12	4,32
IOZ09422	大约是东北	modern	Lynx lynx	10,5	8,82	23,38	0,84	2,227	12,94	7,08	10,92	0,547	0,844	20,32	9,24	7,22	4,24
IOZ08120	吉林安？	modern	Lynx lynx	9,52	7,32	21	0,769	2,206	12	6,32	10	0,527	0,833	19,02	9,32	6,8	4,36
IOZ08120	吉林安？	modern	Lynx lynx	8,84	7,12	20,2	0,805	2,285	11,74	6,32	9,72	0,538	0,828	18,84	9,22	6,74	4,02
IOZ09419	大约是东北	modern	Lynx lynx	10,02	7,9		0,788		12,18	6,68		0,548		19,42	9,32	7	4,02
IOZ09419	大约是东北	modern	Lynx lynx	10	8,08		0,808		12,06	6,56		0,544		19,4	9,38	6,98	4,04
IOZ T0139	西藏	modern	Lynx lynx	8,28	6,68		0,807		11,38	6,02	9,76	0,529	0,858	18,72	8,72	6,48	3,54
IOZ T0139	西藏	modern	Lynx lynx	8,12	6,58		0,81		11,34	6,02	9,82	0,531	0,866	18,84	8,58	6,48	4
IOZ T0138	西藏	modern	Lynx lynx	8,76	7,42		0,847		12,52	7,04		0,562		19,62	9,12	6,34	4,1
IOZ T0138	西藏	modern	Lynx lynx	9	7,32		0,813		12,54	6,92		0,552		19,52	9,02	6,38	4,02
IOZT0323	西藏	modern	Lynx lynx	7,65	6,48		0,847		10,33	5,25	6,93	0,508	0,671	16,69	8,24	5,51	3,74
IOZT0323	西藏	modern	Lynx lynx	7,89	6,45		0,817		10,6	5,6	7,27	0,528	0,686	16,64	8,38	5,6	3,96
USNM152619	Spain, Huel	modern	Lynx pardinus	7,47	6,27	15,79	0,839	2,114	10,52	5,08	8,17	0,483	0,777	16,1	7,56	5,97	2,95
USNM152619	Spain, Huel	modern	Lynx pardinus	7,39	6,37	17,67	0,862	2,391	9,92	5,26	8,53	0,53	0,86	15,98	7,26	5,78	3,39
USNM152618	Spain, Huel	modern	Lynx pardinus	7,39	5,99	17	0,811	2,3	10,18	4,92	8,49	0,483	0,834	14,49	6,96	5,49	2,77
USNM152618	Spain, Huel	modern	Lynx pardinus	7,25	5,66	16,98	0,781	2,342	10,06	5,03	8,66	0,5	0,861	14,36	6,95	5,37	3,05
AMNH M169492	Spain, Tole	modern	Lynx pardinus	7,26	5,9		0,813		10,11	5,01		0,496		15,47	7,34	5,6	2,9
AMNH M169492	Spain, Tole	modern	Lynx pardinus						10,09	4,97		0,493		15,34	7,53	5,7	3,1
USNM81910	Washington	modern	Lynx canadensis	7,4	5,92	17,89	0,8	2,418	10,8	4,96	8,36	0,459	0,774	16,49	7,62	5,6	4,08
USNM81910	Washington	modern	Lynx canadensis	7,69	5,96	18,88	0,775	2,455	10,15	4,8	8,1	0,473	0,798	16,46	7,66	5,22	4,31
USNM77095	Washington	modern	Lynx canadensis	6,58	4,93	17,13	0,749	2,603	9,4	4,61	7,86	0,49	0,836	15,1	7,07	5,19	3,57
USNM77095	Washington	modern	Lynx canadensis	6,41	5,09	15,94	0,794	2,487	9,53	4,45	7,7	0,467	0,808	15,4	6,89	4,97	3,87
USNM212611	Yukon	modern	Lynx canadensis	8,39	6,22	20,77	0,741	2,476	10,99	5,38	9,26	0,49	0,843	17,17	7,89	5,77	3,64
USNM212611	Yukon	modern	Lynx canadensis	8,26	6,21	21,3	0,752	2,579	10,78	5,47	9,1	0,507	0,844	16,94	7,74	5,74	3,92
USNM212620	Yukon	modern	Lynx canadensis	7,06	5,67		0,803		10,71	4,95	8,62	0,462	0,805	16,8	8,13	5,29	3,88
USNM212620	Yukon	modern	Lynx canadensis	7,08	5,59	18,51	0,79	2,614	10,92	5,11	8,84	0,468	0,81	16,72	7,93	5,29	4,05
USNM212617	Yukon	modern	Lynx canadensis	7,45	5,61	18,06	0,753	2,424	10,7	5,1	8,42	0,477	0,787	16,8	7,83	5,57	3,99
USNM212617	Yukon	modern	Lynx canadensis	7,26	5,62	18,18	0,774	2,504	10,77	5,16	8,82	0,479	0,819	16,71	7,97	5,69	4,11
USNM33126	Minnesota	modern	Lynx canadensis	7,69	5,98		0,778		10,27	5,25	9,26	0,511	0,902	16,58	7,59	5,77	3,3
USNM33126	Minnesota	modern	Lynx canadensis	7,4	5,98		0,808		10,58	5,43	9,51	0,513	0,899	16,49	7,63	5,84	3,66
AMNH11802	Ark. 15 Mi	modern	Lynx canadensis						8,42	5	7,02	0,594	0,834	13,97	6,15	4,45	3,22
USNM224357	Oregon	modern	Lynx rufus														
USNM224357	Oregon	modern	Lynx rufus														
USNM224359	Oregon	modern	Lynx rufus														
USNM224359	Oregon	modern	Lynx rufus														
USNM224342	Oregon	modern	Lynx rufus														
USNM224342	Oregon	modern	Lynx rufus														
USNM225357	Oregon	modern	Lynx rufus														
USNM225357	Oregon	modern	Lynx rufus														
AMNH M14822	Texas	modern	Lynx rufus	6,92	5,82	16,29	0,841	2,354	9,53	5,26	7,78	0,552	0,816	15,29	6,82	6,01	2,86
AMNH M14822	Texas	modern	Lynx rufus	6,6	5,89	16,21	0,892	2,456	9,65	5,07	8,07	0,525	0,836	15,12	7,15	6,03	2,73
AMNH M14823	Texas	modern	Lynx rufus	6,92	5,24		0,757		9,04	4,53	7,45	0,501	0,824	13,59	6,03	5,09	2,4
AMNH M14823	Texas	modern	Lynx rufus	6,63	5,46	15,52	0,824	2,341	9,14	4,57	7,51	0,5	0,822	13,97	6,2	5,28	2,68
AMNH M243108	Florida	modern	Lynx rufus	7,51	6,6	17,64	0,879	2,349	9,42	5,16	7,87	0,548	0,835	14,4	7,28	5,87	2,36
AMNH M243108	Florida	modern	Lynx rufus	7,27	6,54	18,66	0,9	2,567	9,36	5,08	7,71	0,543	0,824	14,51	7,08	5,86	2,57
AMNH M24666	Mexico，S	modern	Lynx rufus	6,04	4,54	14,28	0,752	2,364	8,53	4,5	6,68	0,528	0,783	13,07	5,93	4,78	2,29
AMNH M24666	Mexico，S	modern	Lynx rufus	5,98	4,45	14,52	0,744	2,428	8,55	4,63	6,97	0,542	0,815	12,68	5,72	4,86	2,52
AMNH M24665	Mexico，S	modern	Lynx rufus	6,28	5,06		0,806		9,2	4,53	6,98	0,492	0,759	13,89	6,6	5,2	2,3
AMNH M24665	Mexico，S	modern	Lynx rufus	6,08	5,06	15,19	0,832	2,498	9,22	4,67	7,43	0,507	0,806	13,8	6,38	5,15	2,47
IOZ23613	云南永德	modern	Catopuma temminckii	9,14	6,52	18,5	0,713	2,024	10,22	6		0,587		16,82	7,58	5,88	3,28
IOZ23613	云南永德	modern	Catopuma temminckii	9,02	6,2		0,687		10,42	6,12	7,72	0,587	0,741	16,7	7,42	5,82	3,18
IOZ25947	湖北房县	modern	Catopuma temminckii	8,64	6,25	17,18	0,723	1,988	10,5	5,33	6,89	0,508	0,656	17,48	8,48	5,93	3,14
IOZ25947	湖北房县	modern	Catopuma temminckii	8,62	6,27	16,94	0,727	1,965	10,86	5,46	7,62	0,503	0,702	17,72	8,44	5,88	3,69
IOZ29533	湖北房县	modern	Catopuma temminckii	6,89	5,34	16,46	0,775	2,389	9,52	5,28	7,62	0,555	0,8	16,52	7,52	5,79	2,85
IOZ29533	湖北房县	modern	Catopuma temminckii	7,01	5,34	16,46	0,762	2,348	9,12	5,28	6,97	0,579	0,764	16,34	7,46	5,63	3,02
IOZ 无号		modern	Catopuma temminckii											18,14	8,72		
IOZ 无号		modern	Catopuma temminckii											18,56	8,52		
IOZ25038	四川平武	modern	Catopuma temminckii	7,18	5,62	14,78	0,783	2,058	10,24	5,12		0,5		16,72	7,52	5,62	3,28
IOZ25038	四川平武	modern	Catopuma temminckii	7,32	5,52	15,24	0,754	2,082	10,48	5,18		0,494		16,46	7,72	5,52	3,24
IOZ23601	四川平武	modern	Catopuma temminckii	7,29	5,73	16,49	0,786	2,262	10,29	5,01		0,487		15,75	7,73	5,38	2,71
IOZ23601	四川平武	modern	Catopuma temminckii	7,26	5,91	17,17	0,814	2,365	10,43	5,19		0,498		15,79	7,72	5,64	2,69
USNM259012	四川汶川	modern	Catopuma temminckii	8,88	6,58		0,741		11,17	6,24	7,64	0,559	0,684	17,76	8,41	5,82	4,3
USNM259012	四川汶川	modern	Catopuma temminckii	8,68	6,61		0,762		10,92	6,17	7,57	0,565	0,693	18,1	8,55	5,91	4,1
USNM182310	Kenya, Ulu	modern	Caracal caracal	8,16	5,95	14,68	0,729	1,799	9,81	4,94	7,45	0,504	0,759	16,15	7,9	5,05	3,18
USNM182310	Kenya, Ulu	modern	Caracal caracal	7,65	5,75	13,95	0,752	1,824	10,16	4,94	7,43	0,486	0,731	16,05	7,8	5,09	3,14
USNM182218	Kenya, Ulu	modern	Caracal caracal	7	4,91		0,701		8,63					15,04	6,73	4,87	2,51
USNM182218	Kenya, Ulu	modern	Caracal caracal	7,17	5,15	13,63	0,718	1,901	8,71					15,36	6,72	4,94	2,64
USNM368503	Botswana	modern	Caracal caracal	8,86	7,07		0,798		11,69					17,61			
USNM368503	Botswana	modern	Caracal caracal						11,88					17,76			
USNM40164	Botswana	modern	Caracal caracal	7,66	5,13	14,83	0,67	1,936	9,02	4,73	7,76	0,524	0,86	16,23	6,77	4,82	2,94
USNM40164	Botswana	modern	Caracal caracal	7,48	5,14	14,43	0,687	1,929	9,07	4,88	7,96	0,538	0,878	15,88	6,95	4,71	2,89
USNM384162	Botswana	modern	Caracal caracal														
USNM384162	Botswana	modern	Caracal caracal														

catalogue	P4MeL	前尖高PH	P4W/L	P4BW/L	P4PL/L	P4ML/L	M1L	M1W	M1W/L	C.P4	P3.P4		L1	L2	L3	LT	W1	W2	W3	LDP
HMV 2010 X1813	5,61		0,495	0,365	0,181	0,386	2,85	5,42	1,902	0,53	0,65	0,373	120,64	114,49	107,91	37,63	88,27	46,46	32,67	
HMV 2010 X1813	5,34		0,492	0,366	0,14	0,364	2,35	5,55	2,362	0,526		0,379				41,01	88,27			8,55
V13539	7,35		0,453	0,323	0,217	0,365														
V13539																		62,89	41,91	7,43
V13540																47,31	97,92	61,24	37,68	7,78
V13540	6,71		0,475	0,343	0,211	0,357										47,16				
HMV2013 X1799			0,48	0,37	0,184					0,563	0,662					48,44		63,1	40,65	8,93
HMV2013 X1799																				
HMV2016 X2126	7,5				0,19	0,388				0,537	0,657		180,48			53,4				9,15
HMV2016 X2126	7,36				0,202	0,378				0,53	0,684					53,35		59,63	42,6	8,32
HMV2015 X1849	7,05				0,218	0,364				0,497			172,42	152,18		50,51	107,62	58,14	45,14	7,74
HMV2015 X1849	6,99				0,234	0,368				0,507	0,68					50,89				8,65
HMV2017 01429																				
HMV2017 01429										0,531	0,623		171,02	151,32		49,95	106,27	60,27	43,96	8,07
HMV2014 X1821										0,48	0,585		166,52	153,82		52,11	113,14	63,89	44,87	8,42
HMV2014 X1821										0,485						49,61				
HMV 2011 X1775	6,89		0,453	0,357	0,156	0,371	4,46	6,76		0,488	0,604	0,364		137,73						
HMV 2011 X1775																				
HMV 2012 X1781	6,31	9,3		0,326	0,174	0,368	3,12	5,71		0,488	0,634	0,333	157,72	137,52		45,82		55,06	39,47	9,58
HMV 2012 X1781	5,76		0,457	0,334	0,193	0,351	2,78	5,55		0,484	0,665	0,338				45,78				9,34
X1812										0,517	0,682					45,64				7,01
X1812											0,621					43,65				5,57
X1868			0,498	0,408						0,603	0,663			145,97		50,68				8,94
X1868																51,87		55,37	39,88	9,02
X1870			0,506	0,38						0,489	0,682					47,63		65,22	44,64	8,09
X1870																				
HMV1230										0,57	0,662		158,82	146,28		50,1	112,69	59,65	42,76	10,46
HMV1230																50,54				9,37
HMV1226	7,16	10,98	0,489	0,356	0,189	0,367	3,31	6,32		0,536	0,664	0,324	161,02	150,91		52,49	110,53	62,66	42,79	9,31
HMV1226	7,29	10,8	0,478	0,351	0,22	0,367		5,83		0,544	0,661	0,294				52,23				10,49
AMNH M4137	6,26	10,69	0,464	0,398	0,193	0,356	3,3	5,96	1,806	0,523	0,653	0,339	135,46	121,35		42,93	93,14	57,68	35,66	4,1
AMNH M4137	5,99	11,01	0,471	0,394	0,201	0,34	3,22	5,96	1,851	0,526	0,658	0,339				43,98				5,06
IOZ08119	7,7		0,471	0,322	0,146	0,375	3,5	6	1,714	0,502	0,59	0,292	158,32	143,22		51,22	116,18	68,62	44,44	5,98
IOZ08119	7,5	11,4	0,469	0,333	0,159	0,362	3,6	6,7	1,861	0,487	0,594	0,323				50,74				6,78
IOZ09426	6,7	10,9	0,497	0,347	0,161	0,347	3,6	6,3	1,75	0,518	0,611	0,326	155,42	142,12		48,22	110	68,42	42,52	6,9
IOZ09426	6,9	11,1	0,487	0,36	0,168	0,35	3,3	6	1,818	0,482	0,589	0,305				48,92				6,8
IOZ07809	8	11,86	0,437	0,326	0,218	0,4	3,92	6,82	1,74	0,426	0,559	0,341	146,28	131,62		45,62	101,42	61,52	38,64	5,92
IOZ07809	7,9	11,38	0,429	0,326	0,21	0,392	3,9	6,8	1,744	0,44	0,584	0,338				45,86				5,9
IOZ09422	7,72	11,5	0,462	0,353	0,214	0,383	4,12	6,16	1,495	0,541	0,639	0,305	163,24	148,82		50,12	116,04	70,08	44,72	6,92
IOZ09422	7,48	12,54	0,455	0,355	0,209	0,368	4,48	7,3	1,629	0,517	0,637	0,359		148,82		49,02				6,68
IOZ08120	6,82	10,72	0,49	0,358	0,229	0,359	4,18	7,18	1,718	0,501	0,631	0,377	148,74	134,52		45,62	108,4	61,52	38,48	6,02
IOZ08120	7,02	11,02	0,489	0,358	0,213	0,373	4,06	7,08	1,744	0,469	0,623	0,376				45,58				6,34
IOZ09419	7,62	11,28	0,48	0,36	0,207	0,392	3,92	7,22	1,842	0,516	0,627	0,372	149,12	135,42		48	105,7	65,1	43,64	7,18
IOZ09419	7,38	11,46	0,484	0,36	0,208	0,38	3,94	7,1	1,802	0,515	0,622	0,366				47,66				6,46
IOZ T0139	6,88	10,62	0,466	0,346	0,189	0,368	3,64	6,96	1,912	0,442	0,608	0,372	134,72	122,34		42,62	95,44	58,76	34,78	4,54
IOZ T0139	6,92	10,86	0,455	0,344	0,212	0,367	3,66	6,76	1,847	0,431	0,602	0,359				42,62				5,4
IOZ T0138	7,18		0,465	0,323	0,209	0,366	4,52	6,42	1,42	0,446	0,638	0,327	142,34	129,54		45,74	100,32	60,92	39,62	4,96
IOZ T0138	7,44	10,52	0,462	0,327	0,206	0,381				0,461	0,642					45,18				4,62
IOZT0323	5,84	8,59	0,494	0,33	0,224	0,35	2,17	4,97	2,29	0,458	0,619	0,298	132,44	121,22		41,42	86,85	52,6	32,99	6,07
IOZT0323	5,69	9,11	0,504	0,337	0,238	0,342	2,12	4,73	2,231	0,474	0,637	0,284				41,36				6,07
USNM152619	6,07	9,25	0,47	0,371	0,183	0,377	2,64	4,85	1,837	0,464	0,653	0,301				39,78		54,14	36,09	5,96
USNM152619	5,67	9,26	0,454	0,362	0,212	0,355	2,76	4,44	1,609	0,462	0,621	0,278				38,78				5,18
USNM152618	5	8,67	0,48	0,379	0,191	0,345				0,51	0,703					36,39		52,36	32,97	4,95
USNM152618	4,83	9,43	0,484	0,374	0,212	0,336	2,31	4,33	1,874	0,505	0,701	0,302	120,11			36,28				4,69
AMNH M169492	5,78	8,27	0,474	0,362	0,187	0,374	2,65	4,26	1,608	0,469	0,654	0,275	131,62	118,86		38,36	93,01	52,66	35,13	5,83
AMNH M169492	5,58		0,491	0,372	0,202	0,364					0,658					38,22				5,74
USNM81910	6,32	8,95	0,462	0,34	0,247	0,383	2,67	4,04	1,513	0,449	0,655	0,245	127,79	118,91		41,09	89,96	54,18	35,39	6,72
USNM81910	5,95	9,26	0,465	0,317	0,262	0,361	2,8	4,52	1,614	0,467	0,617	0,275				40,41				6,76
USNM77095	5,79	8,5	0,468	0,344	0,236	0,383	2,24	4,19	1,871	0,436	0,623	0,277	123,82	113,61		37,62	87,22	52,11	32,94	6,83
USNM77095	5,73	8,69	0,447	0,323	0,251	0,372	2,28	4,45	1,952	0,416	0,619	0,289				37,8				6,75
USNM212611	6,47	9,71	0,46	0,336	0,212	0,377	2,84	5,21	1,835	0,489	0,64	0,303	134,28	121,83		41,97	95,06	57,77	36,73	6,03
USNM212611	6	10,05	0,457	0,339	0,231	0,354	3,09	5,24	1,696	0,488	0,636	0,309				42,02				6,86
USNM212620	6,61	9,18	0,484	0,315	0,231	0,393	2,86	5,12	1,79	0,42	0,638	0,305	130,5	119,52		39,86	90,15	53,16	35,56	6,55
USNM212620	6,36	9,54	0,474	0,316	0,242	0,38	3,19	5,36	1,68	0,423	0,653	0,321				39,82				6,51
USNM212617	6,49	8,92	0,466	0,332	0,238	0,386	3,07	4,82	1,57	0,443	0,637	0,287	127,68	121,02		40,01	90,65	54,05	33,54	5,61
USNM212617	6,24	10,06	0,477	0,341	0,246	0,373	2,91	5,02	1,725	0,434	0,645	0,3				40,41				5,61
USNM33126	6,61	9,71	0,458	0,348	0,199	0,399	2,7	4,24	1,57	0,464	0,619	0,256	135,05	124		40,72	96,85	55,62	36,49	6,36
USNM33126	6,19	9,97	0,463	0,354	0,222	0,375	2,63	4,57	1,738	0,449	0,642	0,277				40,63				5,89
AMNH11802	5,14	7,28	0,44	0,319	0,23	0,368					0,603									
USNM224357																				
USNM224357																				
USNM224359																				
USNM224359																				
USNM224342																				
USNM224342																				
USNM225357																				
USNM225357																				
AMNH M14822	5,96	7,97	0,446	0,393	0,187	0,39	3,73	6,01	1,611	0,453	0,623	0,393	124,25	113,12		36,62	81,97	49,52	33,57	5,04
AMNH M14822	5,63	8,27	0,473	0,399	0,181	0,372	3,14	5,63	1,793	0,437	0,638	0,372				36,87				5,29
AMNH M14823	4,98	7,86	0,444	0,375	0,177	0,366	2,37	3,84	1,62	0,509	0,665	0,283	119,02	109,42		35,29	80,61	47,13	29,97	6,29
AMNH M14823	4,68	8,3	0,444	0,378	0,192	0,335	2,24	4,26	1,902	0,475	0,654	0,305				35,21				5,47
AMNH M243108	5,36	8,34	0,506	0,408	0,164	0,372	2,47	4,83	1,955	0,522	0,654	0,335	131,11	120,07		37,62	89,99	52,71	34,97	6,45
AMNH M243108	5,17	8,51	0,488	0,404	0,177	0,356	2,52	4,86	1,929	0,501	0,645	0,335				37,62				6,43
AMNH M24666	4,78	7,51	0,454	0,366	0,175	0,366	2,15	3,86	1,795	0,462	0,653	0,295	115,88	105,03		33,86	77,18	46,39	28,47	5,83
AMNH M24666	4,36	7,59	0,451	0,383	0,199	0,344	2,24	4,13	1,844	0,472	0,674	0,326				33,68				5,93
AMNH M24665	5,03	8,12	0,475	0,374	0,166	0,362	2,35	4,58	1,949	0,452	0,662	0,33	133,19	118,04		37,89	87,44	49,26	31,72	8,27
AMNH M24665	4,79		0,462	0,373	0,179	0,347	2,31	4,83	2,091	0,441	0,668	0,35				37,81				8,46
IOZ23613	6,02	9,12	0,451	0,35	0,195	0,358	2,72	5,18	1,904	0,543	0,608	0,308	144,88	129,66		43,72	94,04	53,72	34,28	9,02
IOZ23613	6,18	9	0,444	0,349	0,19	0,37	2,68	5,2	1,94	0,54	0,624	0,311				43,74				8,32
IOZ25947	6,42	8,62	0,485	0,339	0,18	0,367	2,42	4,73	1,955	0,494	0,601	0,271	138,12			42,57	86,7	54,22	33,09	5,92
IOZ25947	6,27	8,72	0,476	0,332	0,208	0,354	2,36	4,49	1,903	0,486	0,613	0,253				42,24				5,57
IOZ29533	5,85	8,25	0,455	0,35	0,173	0,354	2,25	4,45	1,978	0,417	0,576	0,269	127,6	115,84		38,42	81,51	48,92	30,35	6,63
IOZ29533	5,88	8,47	0,457	0,345	0,185	0,36	2,42	4,89	2,021	0,429	0,558	0,299				39,13				7,2
IOZ 无号			0,481																	
IOZ 无号			0,459																	
IOZ25038	6,12		0,45	0,336	0,196	0,366				0,429	0,612		130,86	117,04		41,18	84,48	51,74	30,78	7,68
IOZ25038	6		0,469	0,335	0,197	0,365				0,445	0,637					40,54				7,56
IOZ23601	5,72		0,491	0,342	0,172	0,363				0,463	0,653		131,4	118,69		40,59	85,35	52,07	30,29	7,45
IOZ23601	5,55		0,489	0,357	0,17	0,351	2,27	4,93	2,172	0,46	0,661	0,312				40,03				7,32
USNM259012	5,99		0,474	0,328	0,242	0,337	2,33	5,16	2,215	0,5	0,629	0,291	154,31	140,76		45,21	102,09	56,28	36,83	8,63
USNM259012	6,33		0,472	0,327	0,227	0,35	2,24	4,54	2,027	0,48	0,603	0,251				44,61				8,07
USNM182310	5,91	8,68	0,489	0,313	0,197	0,366	2,81	4,67	1,662	0,505	0,607	0,289	131,98	119,5		39,52	87,65	49,58	31,04	5,49
USNM182310	5,61	9,1	0,486	0,317	0,196	0,35	2,85	4,74	1,663	0,477	0,633	0,295				39,3				6,01
USNM182218	5,41	8,34	0,447	0,324	0,167	0,36	2,39	4,1	1,715	0,465	0,574	0,273	117,18	106,63		36,67	82,13	48,57	30,83	5,57
USNM182218	5,55	8,26	0,438	0,322	0,172	0,361				0,467	0,567					36,59				5,76
USNM368503								5,11		0,503	0,664	0,29	150,88	136,46		45,04	109,73	58,96	41,68	6,44
USNM368503								5,44			0,669	0,306				45,21				6,53
USNM40164	6,32	8,86	0,417	0,297	0,181	0,389	2,57	4,18	1,626	0,472	0,556	0,258	120,97	110,36		37,37	80,53	48,17	28,44	4,97
USNM40164	5,99	9,04	0,438	0,297	0,182	0,377	2,41	4,7	1,95	0,471	0,571	0,296				37,36				4,94
USNM384162																				
USNM384162																				

Appendix for

A small *Lynx* from Longdan, Gansu Province and the diversification of *Lynx* lineage during the Plio-Pleistocene

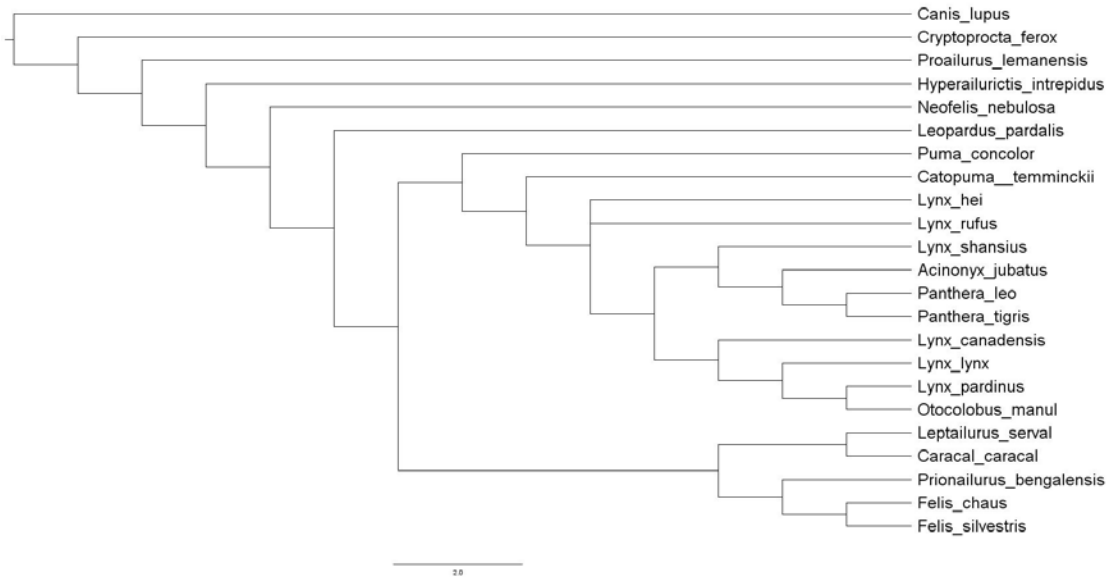

Fig. S1. Maximum parsimony analysis, without constraint.

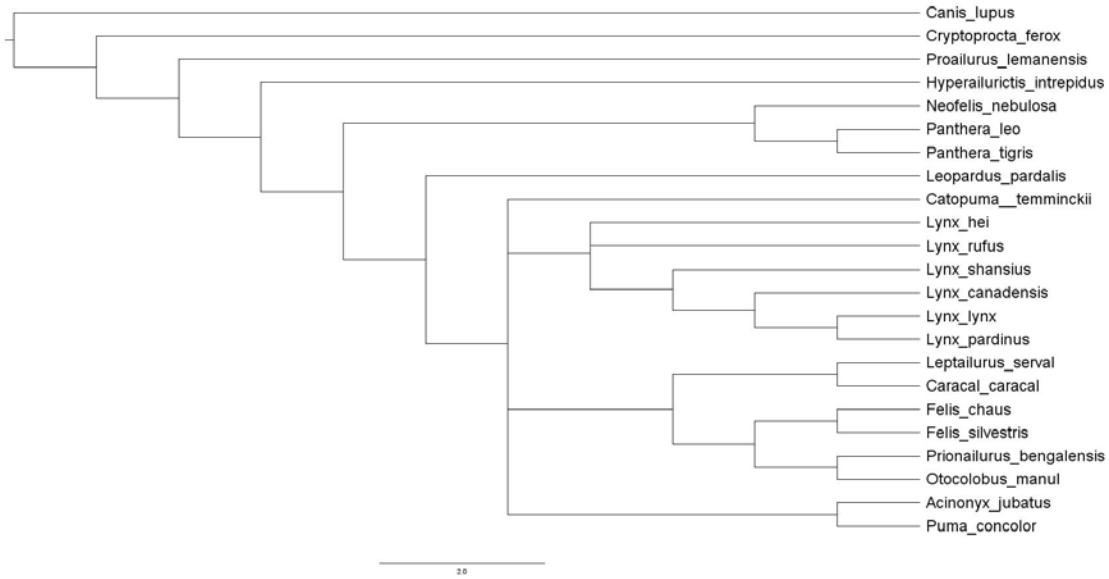

Fig. S2. Maximum parsimony analysis, with constraint on *Panthera* with *Neofelis*, *Acinonyx* with *Puma*, and *Otocolobus* with *Prionailurus*.

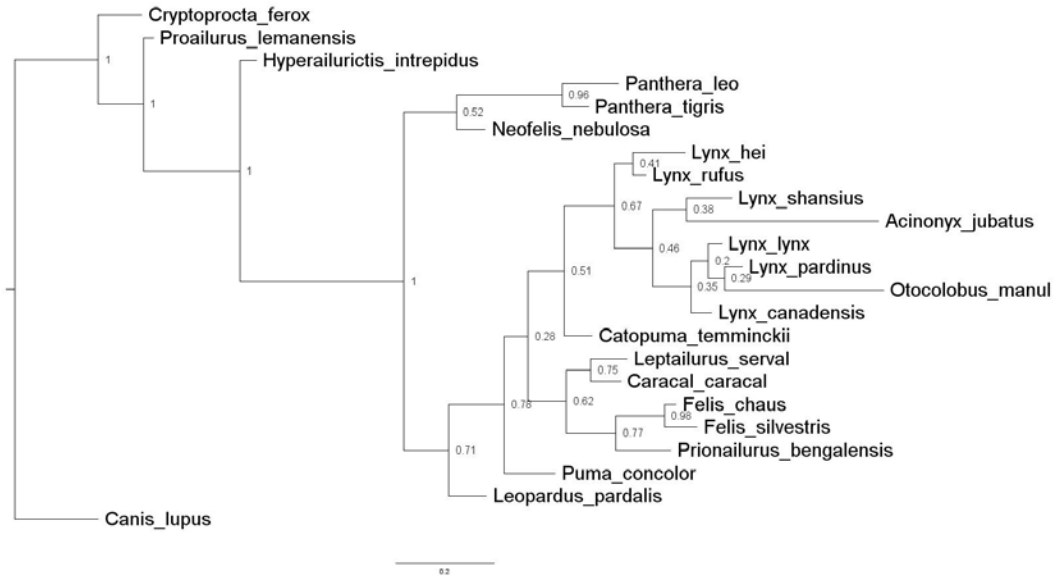

Fig. S3. Bayes Inference analysis, without constraint.

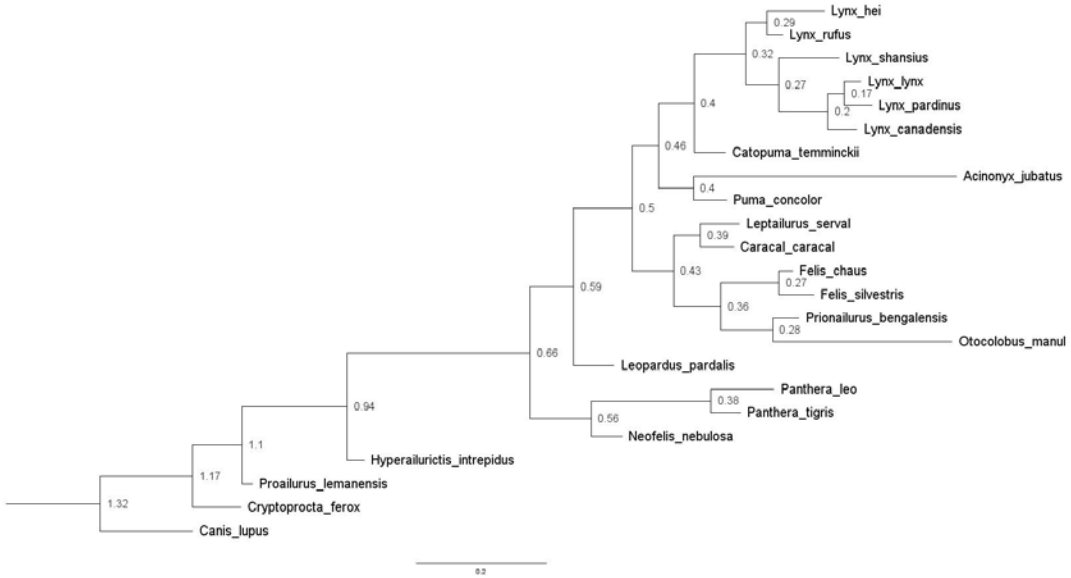

Fig. S4. Bayes Inference analysis, with constraint on *Acinonyx* with *Puma*, and *Otocolobus* with *Prionailurus*.

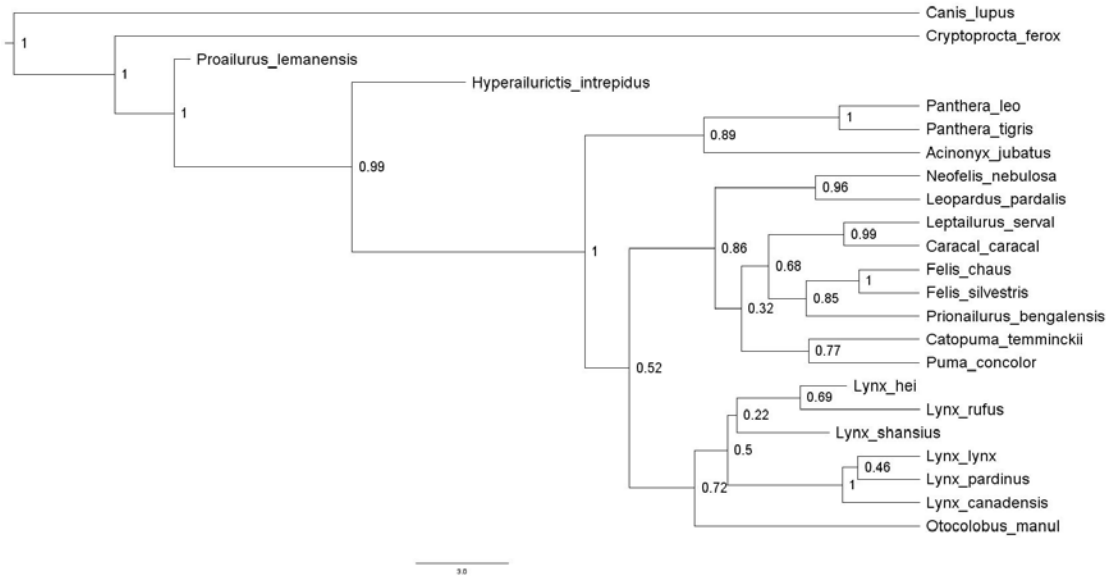

Fig. S5. Bayes Inference tip-dating analysis, without constraint.

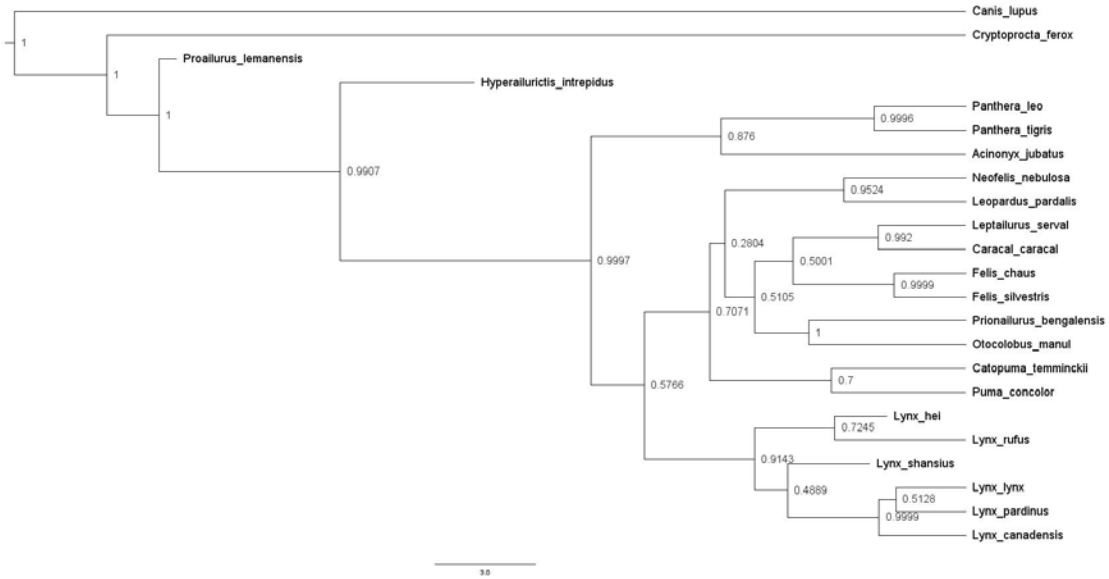

Fig. S6. Bayes Inference tip-dating analysis, with constraint on *Otocolobus* with *Prionailurus*.